Fermilab Library
0 1160 0031346 4

Massachusetts Institute of Technology

ASTROPHYSICS

FERMILAB
SEP 27 1993
LIBRARY

Submitted to *The Astrophysical Journal*
July 15, 1993

PREDICTIONS OF A POPULATION OF CVs IN GLOBULAR CLUSTERS

R. Di Stefano[1,2,3] and S. Rappaport[1]

MIT, LNS

Preprint Series No. CSR-93-08

[1]Department of Physics, Massachusetts Institute of Technology, Cambridge, Massachusetts 02139

[2]*Address after September 1, 1993*: Harvard-Smithsonian Center for Astrophysics, 60 Garden Street, Cambridge, MA 02138

[3]On leave from the Department of Physics, New York Institute of Technology, Old Westbury, NY 11568

Department of Physics
Department of Mathematics
Department of Earth, Atmospheric, and Planetary Sciences
Center for Space Research
Center for Theoretical Physics
Research Laboratory of Electronics

ABSTRACT

We have studied the number of cataclysmic variables that should be active in globular clusters during the present epoch due to binary formation via two-body tidal capture. In particular, we predict the orbital period and luminosity distributions of cataclysmic variables (CVs) in globular clusters. The results are based on Monte Carlo simulations combined with evolution calculations appropriate to each system formed during the lifetime of two specific globular clusters, ω Cen and 47 Tuc. From our study of these two clusters, which represent the range of core densities and states of mass segregation that are likely to be interesting, we extrapolate our results to the Galactic globular cluster system. Although there is at present little *direct* observational evidence of CVs in globular clusters, we find that there should be a large number of active systems.

In particular, we predict that there should be more than $\sim$ 100 CVs in both 47 Tuc and ω Cen, and several thousand in the Galactic globular cluster system. These numbers are based on two-body processes alone and so represent a lower bound on the number of systems that may have been formed due to stellar interactions within globular clusters.

The relation between these calculations and the paucity of optically detected CVs in globular clusters is discussed. Moreover, some of these predictions should be testable in future optical and UV studies with HST, and X-ray studies with the present and future generations of X-ray detectors. Should future observations fail to find convincing evidence of a substantial population of cluster CVs, then the two-body tidal capture scenario is likely to be seriously constrained.

Of the CVs we expect in 47 Tuc and ω Cen, approximately 45 and 20, respectively, should have accretion luminosities above 10^{33} ergs s^{-1}. However, if one utilizes a relation for converting accretion luminosity to hard X-ray luminosity that is based on observations of Galactic plane CVs, then even these sources will not exhibit X-ray luminosities above 10^{33} ergs s^{-1}. Thus, while we cannot *directly* account for the most luminous subset of the low-luminosity globular cluster X-ray sources ($10^{33} - 10^{34.5}$ ergs s^{-1}) without assuming an evolutionary pattern that is different from the majority of CVs in the disk, we are able to account for all of the observed lower-luminosity subset of these sources ($10^{31.5} - 10^{33}$ ergs s^{-1}), many of which have been recently discovered through Rosat observations. Futhermore, we find that in order for our predicted *integrated* cluster X-ray luminosities to be consistent with observational upper limits, the relation between accretion and X-ray luminosities should indeed be something like that inferred from the Galactic plane population of CVs. Finally, our calculations predict a large number of very low-luminosity CVs ($L_{acc} < 10^{32}$ ergs s^{-1}) that should be detectable in future optical and X-ray observations.

1. Introduction

Close encounters between single stars are expected to occur regularly within a few core radii of the dense central regions of globular clusters. When two stars pass within a few stellar radii of each other, tidal distortions may absorb enough energy to allow the stars to become bound together in a binary system—i.e., they may undergo a tidal capture (see, e.g., Fabian, Pringle, & Rees 1975; Press & Teukolsky 1977; Lee & Ostriker 1986; McMillan, McDermott, & Taam 1987). When one of the interacting stars is a white dwarf, the resulting binary system may subsequently begin an epoch during which mass is transferred from the extended star to the white dwarf; i.e., it becomes a CV. The total number of binaries containing white dwarfs, formed through two-body tidal capture during the lifetime of the cluster, may be large. The question addressed in this paper is: in what fraction of these systems is mass transfer occurring at the present time, and what is the mass tranfer rate, luminosity, and binary period?

We have used the observation-based models of Meylan (1987, 1989) to carry out calculations for two specific clusters, ω Cen, and the relatively more centrally dense 47 Tuc, which is also more relaxed and hence exhibits a greater degree of mass segregation. The results can be scaled to apply to other clusters and to the galactic globular cluster system as a whole. Observations with the Hubble Space Telescope and with Rosat are beginning to test these predictions, which yield a lower limit on the number of CVs that should be observed. Should these observations reveal the presence of a number of systems which is significantly larger than the number predicted by tidal capture alone, this would be an indication that primordial binaries (either through their own evolution or through three- and four- body processes) also play an important role in the formation of CVs in globular clusters (see, e.g., Leonard 1989; Hut et al. 1992 and references therein).

Until now, what has been puzzling about the results of searches of globular clusters for CVs, is that so *few* systems have been found. At this point there is probably only one confirmed CV in a globular cluster; this is V101 in M5 (Margon, Downes, & Gunn 1981, Machin et al. 1990). Recently a faint, variable, and very blue object has been located in the error box of X0021.8-7221, a low luminosity X-ray source in 47 Tuc (Auriére et al. 1989, Paresce et al 1992). In addition, there have been reports of a handful of classical novae associated with globular clusters (see, e.g., Sawyer-Hogg & Wehlau 1964). This small number of identifications contrasts sharply with the larger number of systems that might have been expected to be present, simply by extrapolating from evidence for close binary systems containing neutron stars. Our calculations indicate that there may be even *more* CVs present than have been previously predicted (Verbunt and Meylan 1988; Davies 1992). Our predictions may nevertheless shed some light on the discrepancy between theoretical expectations and observations to date, since we find that the large majority of active systems have extremely low luminosities ($L \lesssim 10^{32} erg\ s^{-1}$). Indeed recent observations

with both Rosat and the HST have begun to find some intriguing evidence of systems that might be CVs. In particular, Rosat observations of nearby globular clusters have discovered evidence for several very low luminosity ($L \lesssim 10^{32}$ ergs s^{-1}) sources within a few core radii of several globular clusters (see, e.g., Cool et al. 1993, Grindlay 1992). HST observations were responsible for the discovery of the optical source in the error box of the low-luminosity X-ray source in 47 Tuc (Paresce et al. 1992). If however, after this new round of observations have been completed and analyzed, there is still a dearth of CVs, then some of our basic assumptions about the conditions within globular clusters, or about the formation or lifetimes of CVs may be brought into question. We therefore attempt to outline clearly our assumptions and to indicate how much (or little) room there is to manuever in from a theoretical standpoint should we continue to be able to identify only very few systems.

The methods that we used to carry out the calculations follow the general approach taken in our previous work on the study of tidal captures by neutron stars in globular clusters (Di Stefano and Rappaport 1992, hereafter DR). It was, however, necessary to incorporate several new features in order to study tidal capture by white dwarfs, and to make predictions on the present state of each system which undergoes a successful tidal capture (i.e., a tidal capture in which the extended star survives, even though it may have experienced some mass loss). Perhaps the most important of these new features is the detailed study of those systems in which, after capture, orbital circularization, and an era of binary and/or stellar evolution, an extended star begins mass transfer onto its white dwarf companion. When the compact object is a neutron star, the X-ray emission that accompanies the mass accretion may play a significant role in the subsequent evolution of the extended star, with the X-ray heating flux incident on the extended star far outshining the emergent flux due to its own nuclear burning. The evolution of such systems is complicated (Hameury, King, & Lasota 1986; Podsialowski 1991; Harpaz and Rappaport 1991; Hameury et al. 1993). Therefore, in DR, we did not attempt to follow the detailed evolution of compact X-ray binaries once the mass transfer commenced. When the compact object is a white dwarf, however, this problem does not arise to the same degree, and it is possible to use a binary stellar evolution code to follow these systems in detail, from the time that mass transfer begins, right up to the present epoch.

We pay particular attention to the stability of the process of mass transfer. Previous work had seemed to indicate that a main-sequence star would have to be considerably less massive than its white dwarf companion if it is to be able to transfer mass to that companion in a stable (as opposed to runaway) process. This would have the implication that only the more massive white dwarfs in globular clusters would be likely to be able to become members of mass transfer systems that might be observed as CVs (Bailyn, Grindlay, & Garcia 1990). However, the expressions for the mass transfer rate (see e.g.,

Rappaport, Joss, & Webbink 1982; Rappaport, Verbunt, & Joss 1983; hereafter, RJW and RVJ, respectively) yield stability limits that depend critically not only on the way in which the extended star responds to mass loss, but also on the behavior of mass that leaves the star. In this work we find that mass transfer can be stable over a larger range of values of m/M, i.e., the mass of the extended star divided by the mass of the white dwarf, than is typically assumed.

Nevertheless, there are systems which do experience unstable mass transfer. These may be candidates for the recently discovered supersoft sources (e.g., Greiner, Hasinger, & Kahabka 1991, van den Heuvel, et al. 1992, Schaeidt, Hasinger & Trümper 1993).

In §2, we outline our approach, briefly sketching those features that are common to the calculations of tidal captures involving neutron stars and white dwarfs (where details may be found in DR), and placing special emphasis on those features that were specifically developed to study white dwarf tidal captures and the further evolution of the resulting binary. The results of the calculations are presented in §3. Section 4 focuses on the predictions of the number of systems that are active at the present time and on their distributions of orbital periods and luminosities. We make predictions for specific globular clusters and scale the results to all Galactic globular clusters. We also address the issue of the detectability of these systems, given the sensitivities of Rosat and of the HST. In Section 5 we summarize our conclusions.

2. The Approach

2.1. Overview

The approach that we used is a Monte Carlo simulation to generate capture events, together with analytic and numerical calculations to follow the subsequent history of each system. The Monte Carlo technique allowed us to consider many individual white dwarfs in the core of a globular cluster, to determine: (i) if they capture a cluster field star and, if they do, (ii) the nature and evolutionary state of the captured star. We explicitly studied the effects of mass loss from the extended star during the processes of capture and circularization and, for those systems which successfully circularized, studied the subsequent evolution of the binary system up to the present epoch.

2.2. Cluster Models

The observation-based models of Meylan (1987, 1989) provide us with the core density of each cluster and with the relative number of stars in each of nine discrete mass classes that are relevant to tidal captures involving white dwarfs (see DR for details). For main-sequence stars we used the relative fraction of stars in, and the root mean square velocity appropriate to, each of the relevant mass classes, in order to model these quantities as continuous functions of the stellar mass for each cluster. For white dwarfs we simply used three discrete mass classes: those centered roughly around $\sim 1.1\ M_\odot$, $0.75\ M_\odot$,

and 0.6 $M_\odot$. Although a continuous distribution of white dwarf masses might have been more realistic, the discrete models that we have chosen to work with are adequate for our purpose. We use the information contained in Meylan's models (1987, 1989) to compute the rates of captures involving white dwarfs in each of these mass classes. These rates are computed for the cluster core region and are expressed in terms of the number of interactions per second per white dwarf. Since mass segregation plays a less important role in capture processes involving white dwarfs than it does in those involving neutron stars, it is necessary to consider interactions that take place outside of the core. The work of Verbunt and Meylan (1988) explored the effects of mass segregation on white dwarf (and on neutron star) tidal capture. For both 47 Tuc and ω Cen, they considered compact objects of four different masses (one corresponding to each mass class that contains white dwarfs, and one [of 1.40 $M_\odot$] appropriate for neutron stars). They explored the fraction of tidal captures effected by each, as a function of distance from the center of the cluster and also as a function of the mass of the captured star. The effects of mass segregation are most pronounced in 47 Tuc. There, for example, only $\sim$ 15% of all captures of 0.12 $M_\odot$ main-sequence stars by 0.6 $M_\odot$ white dwarfs take place within one core radius of the center, while $\sim$ 70% of all captures of 0.76 $M_\odot$ giants by 1.1 $M_\odot$ white dwarfs take place within one core radius. We have used the results of Verbunt and Meylan to extrapolate our calculation of the number of capture events within one core radius of each cluster to the cluster as a whole.

The number of systems formed depends on the capture rate per white dwarf and on the number of white dwarfs available to participate in tidal captures. Since our calculations depend directly on the number of white dwarfs of each mass class in the core, we are required to estimate those numbers. A direct approach is to multiply the central stellar density given by Meylan, the fractional number of stars in the relevant mass classes (see RPV), and the volume of the core. This leads, for example, to an estimate of $\sim$ 2500 white dwarfs of mass $\sim$ 1.1 $M_\odot$ in the core of 47 Tuc. The number of white dwarfs in the other classes can be obtained by using the relative numbers given by Meylan to scale from this single mass class, as indicated in Table 1. For ω Cen, the same calculation leads to an estimate of almost 10^5 white dwarfs of mass $\sim$ 1.1 $M_\odot$. We have chosen to scale our results to a more conservative (but arbitrary) estimate of $\sim$ 25,000 white dwarfs of mass 1.1 $M_\odot$. Similarly, the scale factors for white dwarfs of other masses in the core of ω Cen are shown in Table 2.

2.3. Capture Rates

The computation of tidal capture rates by neutron stars in both 47 Tuc and ω Cen, has been discussed in detail in DR. The rates of capture by white dwarfs are calculated in a way that exactly parallels those computations. The results for 47 Tuc are presented in Table 1; Table 2 summarizes the results for ω Cen. In both tables, the first column lists

the white dwarf masses for which the calculations were done. The first three rows apply to the capture of giants, while the second three rows apply to the capture of main-sequence stars.

The second column lists the rates of capture in the core of the cluster by a single white dwarf in the appropriate mass class. Given these rates, the number of captures that can be expected to occur during the cluster lifetime depends on the number of white dwarfs that populate the cluster. As discussed above, the exact numbers are not known. The relative numbers of white dwarfs of different masses, taken from Rappaport, Putney, & Verbunt (1989), and based on the observational work by Meylan (1987, 1989), are listed in the third column. The fourth column lists an enhancement factor, based on the study of mass segregation in these two clusters by Verbunt and Meylan (1988). It is used to get a rough estimate of the number of events expected in the cluster as a whole, given the number that occur within the core. It is given by the reciprocal of a function, $f(m, M)$, which is the fraction of all capture events involving an extended star of mass m and a white dwarf of mass M that occur within one core radius of the center of the cluster. For the purposes of this table, an average over m has been performed. The fifth column lists the number of captures that can be expected to take place in the cluster as a whole during its lifetime, which we have taken to be 15 billion years. This number is the product of the rate of capture in the core, the age of the cluster, the average cluster factor (to extrapolate to the cluster as a whole), and the number of white dwarfs in the appropriate mass class expected to reside in the core. As mentioned in §2.2, this last number is unknown, hence we have scaled our results to 2,500 white dwarfs of mass 1.1 $M_\odot$ in the core of 47 Tuc, and 25,000 white dwarfs of this mass in ω Cen. These numbers reflect the total number of capture events that can be expected to take place before the present epoch.

If we define $\mathcal{N}_{Tuc}$ to be the ratio of the actual number of 1.1 $M_\odot$ white dwarfs in the core of 47 Tuc to 2,500, then $\sim 1000\mathcal{N}_{Tuc}$ giants experience a capture or collision with a white dwarf during the cluster lifetime, while $\sim 300\mathcal{N}_{Tuc}$ main-sequence stars experience such a capture. Similarly, for ω Cen, we define $\mathcal{N}_{Cen}$ to be the ratio of the actual number of 1.1 $M_\odot$ white dwarfs in the core of ω Cen to 25,000. There are $\sim 140\mathcal{N}_{Cen}$ giant captures, and $\sim 270\mathcal{N}_{Cen}$ main-sequence captures in ω Cen.

Active CVs are associated with a subset of these events that successfully form binary systems, subsequently experience an epoch of stable mass transfer, and are still active, and hence potentially observable, today.

2.4. Capture, Mass Stripping, and Circularization

As in DR, we use the cluster characteristics and the computed rates as the input for a Monte Carlo simulation which generates the capture events. For each white dwarf, we generate the time of capture. We then go on to consider only those captures which have taken place before the present epoch. For each of these, the characteristics of the extended

star involved in the capture (its mass if it is a main-sequence star, its core mass if it is a giant), and the distance of closest approach, are generated. If the distance of closest approach is less than one stellar radius, we record the event as a direct collision, but, because of present uncertainties in our understanding of the system's further development, we do not attempt a detailed analysis. For systems which have not experienced a direct collision, we now have enough information to proceed.

We expect mass to be stripped from the extended star in most tidal captures. Mass will continue to be stripped from the target as the binary system circularizes. Since neither analytic calculations nor hydrodynamic simulations have yet been able to formulate reliable estimates of the amount of mass stripped during capture and circularization, we use the work of DR to make an ansatz for the maximum amout of mass that is likely to be stripped. This estimate is based on the amount of matter that is present in the "Roche shell" at the time of closest approach during capture. (See DR for details.) For each capture, we assume that a certain fraction ξ of the mass in the Roche shell is ejected from the system. We carry out simulations for three different values of ξ (0.0, 0.5, and 1.0). Although mass stripping does affect the subsequent evolution of the system, the results are not very sensitive to the precise amount of matter stripped; therefore we sampled the range $0 < \xi < 1$ in only a few steps. The results *are* sensitive to the behavior of the mass that is stripped from the surface of the extended star. More precisely, the results are highly dependent on how the angular momentum balance of the system is affected by the behavior of this mass after it leaves the captured star. The less angular momentum carried away by matter exiting the system, the greater the radius of the final circularized orbit. We have run our simulations for three different angular momentum loss scenarios.

Once the orbit has been successfully circularized, the two stars are well enough separated that the extended star is not overfilling its Roche lobe. (In fact, if the extended star *is* overfilling its Roche lobe, then we question the viability of that system and record it for our tabulations, but do not follow it further.)

Perhaps the greatest source of uncertainty in these calculations comes from gaps in our present understanding of what fraction of tidal capture systems are likely to survive the capture and circularization process. The amount of energy that must be absorbed by the envelope of the extended star during capture and circularization may be a significant fraction of its binding energy, particularly for close first approaches. It has therefore been conjectured that, in some subset of tidal captures, the star will respond by swelling to the point where it might engulf its new compact companion (see, e.g., Ray, Kembhavi, & Antia 1987). It has also been conjectured that (especially in the case of giants), all approaches close enough to trigger a tidal capture are close enough to cause mass to be stripped, and may therefore be potentially fatal to the extended star (see, e.g., Bailyn 1988). In fact SPH simulations verify that mass stripping is a common phenomenon after

close approaches (see, e.g., Rasio & Shapiro 1990, 1991; Davies, Benz, & Hills 1991, 1992, 1993). However, the amount of mass stripped during the first few orbits appears to be small (i.e., significantly smaller than the amount of mass loss that we have allowed for in our simulations) for situations when the first approach is greater than ~ 1.5 stellar radii. It is not yet possible for the SPH simulations to follow the entire process of circularization. However, analytic calculations which take non-linear effects into account also indicate that mass loss will occur during most tidal captures (see, e.g., Kochanek 1992).

We have pointed out (DR) that mass loss need not be fatal to the process of capture and circularization. In fact, it may enhance the probability of a successful circularization. First of all, mass which is ejected from the system requires an input of energy which would otherwise need to be dissipated within the envelope of the extended star. In addition, the change in the system's reduced mass which is associated with mass loss from the extended star may in some cases lead to a larger circularized orbit. These issues and more complete references to the relevant literature are discussed in DR.

However, whether any particular system survives capture and circularization depends on details of its evolution which are beyond the scope of this work. The prescription that we have developed has the effect of eliminating many systems that did not collide, but which experienced close approaches and seem more likely to experience spiral-in than circularization. Whether this elimination is as demanding as nature itself remains to be seen.

2.5. Evolution of the Circularized Binaries

2.5.1. Establishing Contact with the Roche Lobe

Roche lobe contact can be established if either the orbital separation shrinks (through the action of a dissipative process such as gravitational radiation or magnetic braking), or if the extended star is a giant and grows to fill its Roche lobe through its own nuclear evolution. We follow each system from circularization until Roche lobe contact is established. If contact is established before the present epoch, then we follow the process of mass transfer through the present epoch. For systems in which the extended star is a main-sequence star, we use the evolution code developed by RVJ, to follow the process of mass transfer. For systems in which the extended star is a giant, we follow the evolution of the giant by numerical integration of eqs. (3.8) and (3.10) in DR, as well as the equations that describe the dynamics of the orbit, in an approach similar to that taken in Webbink, Rappaport & Savonije (1983), and Joss and Rappaport (1983) [hereafter WRS & JR, respectively]. In the end, we are able to determine the present-day rate of mass transfer as well as the orbital period of the binary.

2.5.2. Mass Transfer

Because the white dwarfs which participate in a tidal capture may be less massive than the extended star, the question of the stability of mass transfer must be carefully

considered. The rate of mass transfer when two stars are in "contact" (i.e., when one of the stars is filling its Roche lobe), can be derived by studying the response of the star to mass loss (does it expand, contract, or maintain the same radius?), and the response of the Roche lobe to the mass transfer within, and mass loss from the system. If the Roche lobe extends relatively deeper into the star as a result of mass loss, then even more mass will be lost, and the mass stripping may become an unstable, or runaway process.

A general expression for the rate of mass transfer was derived in RVJ:

$$\frac{\dot{m}}{m} = \frac{-[\frac{1}{2}\left(\frac{\dot{r}}{r}\right)_{ev} - \left(\frac{\dot{J}}{J}\right)_{gr} - \left(\frac{\dot{J}}{J}\right)_{mb}]}{D}, \tag{2.2.a}$$

where $\dot{r}$ is the time derivative of the extended star's radius due to thermal losses (or gains) or nuclear evolution; the second and third terms in the numerator correspond to the loss of orbital angular momentum due to gravitational radiation and to magnetic braking (see, e.g., Verbunt & Zwann 1980), respectively; and D is a dimensionless denominator described next. In general, D is a function of the mass ratio ($q = M/m$); the fraction of the mass lost by the donor star that remains in the system (β); and α, the ratio of the specific angular momentum carried away by any mass that is ejected ($\frac{dJ_{ej}}{dm_{ej}}$), to a specific angular momentum associated with the orbit, defined as $a^2\omega$, where a and ω are the orbital separation and angular frequency, respectively. The form of the denominator is

$$D = \frac{5}{6} + \frac{\xi_{ad}}{2} - \frac{(1-\beta)}{3(1+q)} - \frac{(1-\beta)\alpha(1+q)+\beta}{q}, \tag{2.2.b}$$

where ξ_{ad} describes the response of the star to adiabatic mass loss, with

$$\xi_{ad} = \frac{d(lnR)}{d(lnM)}. \tag{2.2.c}$$

Since, in the situation that we are considering, net mass can only be lost (not gained) from the extended star, $\dot{m}$ must be negative. Therefore the term in brackets in the numerator and the denominator must be of the same sign. Stability requires both to be positive. Therefore the condition for stability may be expressed as

$$D \geq 0. \tag{2.3}$$

This condition leads to a limit on the ratio m/M (i.e., $1/q$) ; when this ratio becomes too large, the mass transfer becomes unstable. The dependence of this condition on β and α has already been noted (see, e.g., RJW, RVJ, Bailyn, Grindlay & Garcia 1990). However, most of the numbers that are quoted in the literature are based on considering the case for β close to unity. In this case, we obtain a relatively low limit on m/M. The limit is

much larger *and can even be* <u>*greater than one*</u>, when the mass lost from the extended star is ejected from the system ($\beta = 0$), and when α is sufficiently small.

Given that the stability of mass transfer depends critically on what happens to the mass that is lost from the extended star, we must determine what the most likely fate of this matter is. Guidelines are provided by detailed work on the accretion of matter onto white dwarfs and the subsequent nuclear burning. See, e.g., Nomoto (1982, 1987); Papaloizou, Pringle, & MacDonald (1982); and Iben (1982). Using these results, as discussed in §§2.4 below, we find that the rates of mass transfer in most of our simulations are such that, the white dwarfs are expected to undergo repeated nova explosions on time scales comparable to the time intervals between steps in our stellar evolution codes, which are described in the next subsection. This would indicate that much of the accreted mass is ejected from the system with a specific angular momentum appropriate to the white dwarf.

In each panel of Figure 1, the denominator D (eq. [2.2.b]) is plotted as a function of the mass of the main-sequence donor star for each of the three white dwarf masses used in our simulations ($M \sim 1.1, 0.75$, and $0.6\ M_\odot$). In turn, for each value of M, there are three plots: (i) $\beta = 1.0$, the case of conservative mass transfer; (ii) $\beta = 0.5$, and α chosen to correspond to the specific angular momentum of the white dwarf, $\alpha_{wd} = (m/M_T)^2$, with $M_T = m + M$; and (iii) $\beta = 0.0$, and $\alpha = \alpha_{wd}$. These plots make it clear that the most stringent limits on m/M are obtained for $\beta = 1$. In this case, a $0.75\ M_\odot$ white dwarf can undergo stable mass transfer only with main-sequence stars with $m \lesssim 0.56\ M_\odot$, while a white dwarf with mass $0.6\ M_\odot$ can undergo stable mass transfer only with main-sequence stars with $m \lesssim 0.36\ M_\odot$. For the case of $\beta = 0$ [with $\alpha = \alpha_{wd}$], a $0.75\ M_\odot$ white dwarf can participate in stable mass transfer with <u>any</u> star likely to be present in the cluster, while a $0.6\ M_\odot$ white dwarf can experience stable mass transfer with most stars in the cluster, up to approximately $0.7\ M_\odot$. Therefore, although it has been postulated that CV formation in globular clusters may be suppressed because of limits imposed by eq. (2.3) (Bailyn, Grindlay, & Garcia 1990), it is likely that such suppression is not the cause of the dearth of CVs discovered so far in globular clusters. Even in the "worst case" scenario ($\beta = 1$), unstable mass transfer would occur in only about one third of all mass-transfer systems.

There is another feature of tidal capture that also makes such suppression seem to be less likely. That is the fact that mass stripping of the extended star is expected to occur in almost all tidal captures (DR). This means that the extended stars which survive capture and circularization have masses that may in general be somewhat smaller than their mass prior to capture.

2.5.3. Evolution Calculations for Systems Undergoing Mass Transfer

Once the non-degenerate star fills its Roche Lobe and matter begins to accrete onto the surface of the white dwarf, we follow the evolution of the binary orbit and the mass

transfer rate in detail. Figure 2, in which the mass transfer rate, $\dot{M}$, is plotted vs. the orbital period, illustrates important features that emerge from the computations. Each track represents the evolution of a system which contains a 1.1 $M_\odot$ white dwarf accreting mass from a companion star which has an initial mass of $\sim$ 0.75 $M_\odot$. For each track, the uppermost point represents the start of the epoch of mass transfer, and the evolution proceeds downward in the figure. The large dots along each track mark logarithmic time steps.

The left-most track (dashed line) is that of a system in which the extended star is on the main-sequence. We adopted an "interrupted magnetic braking model" (see, e.g., RVJ; Spruit & Ritter 1983; Hameury et al. 1988) to allow for the "period gap" (at $\sim 2-3$ hours) observed in the distribution of the orbital periods of CVs. In this scenario, the magnetic braking is assumed to terminate abruptly when the secondary becomes completely convective. Thus, we see that the evolutionary track for a binary containing a main-sequence star ends abruptly at a point when the orbital period is $\sim$ 3.1 hours, and the mass transfer rate is $\sim 1.3 \times 10^{-9} M_\odot$ yr^{-1}. Mass transfer stops for an interval of some 4×10^8 years, until the orbital separation has decreased sufficiently (this time through the action of gravitational radiation) for the companion to once again fill its Roche lobe. At this point the orbital period is $\sim$ 2.4 hours, and the rate of mass transfer, now driven by the slower dissipation associated with gravitational radiation, is smaller by more than an order of magnitude. The system is said to have passed through the "period gap". For more than 3×10^9 years the orbital period continues to decrease and the rate of mass transfer continues to decline until the period reaches a minimum of slightly more than one hour. At this point, when the secondary has become substantially degenerate, the orbital period begins to increase, while the mass transfer rate continues to decline.

The mass transfer rate of the system is so low, that mass transfer can continue for a Hubble time. Consequently, all systems which consist of a main-sequence star and a white dwarf, and which have begun mass transfer during the history of the cluster, should be active today, with the exception of systems that are presently in the period gap. With sensitive enough instuments we may therefore be able to observe them, in spite of their low luminosity.

Although the evolution of just one system is shown, it typifies the evolution of systems that contain main-sequence stars. If the initial mass of the star is smaller than 0.75 $M_\odot$ (but greater than $\sim$ 0.4 $M_\odot$), the corresponding track will approximately coincide with the one shown here, but will start farther down (i.e., with lower luminosity). If the mass of the star is less than $\sim$ 0.4 $M_\odot$, then the star will be fully convective even at the start of mass transfer, and therefore magnetic braking would not play any role in the evolution of the system (at least not according to the assumptions made in this model). The track of this lower mass system will also match onto the track shown in Figure 2, but will

start in the period gap, at an orbital period of $\sim$ 2.9 hours, and will stretch out more or less horizontally to meet the post-period-gap leg of the track shown. If the accreting white dwarf is less massive than 1.1 $M_\odot$, the evolutionary track will have a position and orientation in the P-$\dot{m}$ plane which is slightly displaced from the track displayed here.

The other tracks shown in Figure 2 correspond to systems in which the extended star is a giant or subgiant. These fan out across the central region of the graph, with each track representing a system in which a $\sim$ 0.75 $M_\odot$ star with a particular value of degenerate core mass starts to transfer mass to its white dwarf companion. Toward the left are the tracks of systems that begin mass transfer when the giant has a small core mass, with the left-most solid track corresponding to an initial core mass of 0.07 $M_\odot$; the initial core mass is incremented by 0.01 $M_\odot$ for each track to the right. These tracks are computed via a simple evolutionary scheme described in DR, WRS, and RJ. Although this evolution scheme is relatively crude, it should provide a reasonable approximation to more sophisticated binary evolution calculations (see, e.g., Iben & Tutukov 1984, Pylyser & Savonije 1988, 1989). In contrast to systems in which the companion is a main-sequence star, these systems have a natural termination point. This occurs when the star has lost its entire envelope, leaving only a degenerate core. For stars which start with a small core mass, mass transfer (driven largely by magnetic braking) dominates the evolution of the system, eating away the envelope until nothing but the core (which may be somewhat more massive than it was at the time that mass transfer began) remains. In these systems, the radius of the star and the orbital period decrease throughout the epoch of mass transfer. For stars that begin mass transfer with cores that are more well developed, the evolution is dominated by the nuclear evolution of the core; in these systems, the stellar radius and the orbital separation continue to increase, even as mass is lost from the giant. The variety of initial core masses leads to a variety of orbital periods and luminosities.

2.5.4. Response of the White Dwarf to Mass Accretion

The details of the dynamical evolution during the era of mass transfer, and, for some values of m/M, even the stability of the process, depend upon the reaction of the white dwarf to the accretion of matter. Will the accreted matter burn steadily, or cyclically, or instead undergo nova explosions and thereby possibly be ejected from the system?

The reaction of a white dwarf to mass accretion, as a function of both the white dwarf mass and $\dot{M}$ has been studied by a number of authors (see, e.g., Nomoto [1982, 1987]; Papaloizou, Pringle, & MacDonald [1982]; and Iben [1982].) Steady accretion is possible only if the rate of mass transfer is either very low (less than $\sim 8 \times 10^{-13} M_\odot$ yr^{-1}) or very high ($\sim 10^{-7} M_\odot$ yr^{-1}). In the systems that are important to this work, the mass transfer rate lies between these two regimes, and the systems are expected to accrete mass for an interval of time (typically $\sim 10^5 - 10^9$ yrs) and then experience an outburst during which all or part of the accreted mass is ejected from the system. The amount of mass that needs

to be accreted before an outburst occurs depends both on M and $\dot{M}$. In the cases that we consider, it is reasonable to assume that most of the mass is ejected. Therefore, in most of our simulations we have made the assumption that β is zero, and that the matter carries with it the specific angular momentum of the white dwarf.

For only a very small fraction of the systems we consider, would the conditions be those required for accretion induced collapse (AIC) of a white dwarf to a neutron star (Bailyn & Grindlay 1990). (We note that the contribution of white dwarf tidal capture to AIC has also been studied by Romani 1990.) We find that only $\sim \frac{1}{6}$ of the white dwarfs would potentially accrete enough matter to increase their overall mass to 1.4 $M_{\odot}$, even for conservative transfer. However, in only a minute fraction of these is the mass transfer rate such as to yield steady nuclear burning. Therefore we do not consider this process further.

3. Calculations and Results

Our results were obtained from Monte Carlo simulations which included roughly 100 to 1000 times as many white dwarfs as are actually expected to be present in the clusters that we studied. Our results are in two forms. The first is a tabular compilation of numbers of capture events, binaries containing white dwarfs, and systems undergoing mass transfer at the present epoch. The second form of presentation consists of plots of the orbital period and luminosity distributions.

3.1. Tabulation of Results

Tables 3 and 4 list the total number of systems that can be expected to be formed and the number that can be expected to be presently active in 47 Tuc and in ω Cen, respectively. The results are given separately for captures which involve a main-sequence star and for captures which involve a giant, since the observable properties of these two classes of system could be quite different. (In order to enhance the statistical precision of the results, the numbers in Tables 3 and 4 were generated with simulations that followed $\sim$ 100 times as many white dwarfs as are expected in each of the two clusters.)

A number of different scenarios were used to explore the effects of mass stripping during circularization. The first column lists the fraction of mass that was assumed to be stripped from the "Roche shell" during circularization (see §2.4 and DR); the fraction, ξ, ranges from 0.0 to 1.0. The second column lists the specific angular momentum that was carried away by the stripped mass, which was assumed to be ejected from the system. For each scenario in which mass was stripped, three values of the specific angular momentum of the ejected mass were considered: zero; the specific orbital angular momentum of the white dwarf; and the specific orbital angular momentum of the companion star.

The results that are presented in the tables are the numbers of capture events; collisions, and catastrophic interactions; systems in which mass transfer begins before the present epoch; and systems in which mass transfer is continuing during the present epoch.

The category of "collisions and catastrophic interactions" (column 5) consists of direct collisions; interactions in which the stars do not physically touch on the first pass, but in which there is so much mass stripped from the extended star that its mass after the interaction is likely to be less than $\sim 0.08\ M_{\odot}$; and interactions in which the distance of closest approach is such that, even after circularization, the extended star would still over-fill its Roche lobe. In column 6, note that all systems which begin mass transfer and in which the white dwarf's companion is a main-sequence star, continue mass transfer to the present day, except for a relatively brief interval (on the order of several hundred million years) during the so-called "period gap".

Given the assumed numbers of white dwarfs in 47 Tuc and ω Cen (see §2.3 and Tables 3 and 4), we expect to find ~ 190 and ~ 145 CVs in these two clusters, respectively, at the present epoch. Of these, 15% (for 47 Tuc) and 3% (for ω Cen) contain giant or subgiant companion stars; the remainder have main-sequence donor stars. One interesting feature of both tables is that the numbers in each category (i.e., each type of event or system, by column) are not dramatically different for different mass loss scenarios (as specified by ξ and j_{ej}). The number of systems that come into contact is maximized for *moderate* mass stripping (at the time of tidal capture; $\xi \cong 0.5$). The reason for this is that mass stripping does allow more systems to successfully circularize because it tends to push the stars apart to the point where the captured star can survive repeated mass stripping on subsequent passages after capture. However, when the mass loss becomes extreme, two effects tend to diminish the number of active mass transfer systems: some of the circularized orbits may be so wide that the systems fail to come close enough for mass transfer to commence within a Hubble time; furthermore, some close approaches may lead to the destruction of the extended star when too much mass is stripped from it in a short time. Overall, differences among the various mass loss scenarios are small, with the ratio between the largest and smallest number of mass transfer systems being smaller than a factor of 2.

Another feature that stands out is the similarity between ω Cen and 47 Tuc in the number of active mass transfer systems that contain main-sequence stars, and the disimilarity in the number of active mass transfer systems that contain giants. Note however that a comparison of the absolute numbers in the tables may be misleading, since these numbers have simply been scaled to the number of white dwarfs estimated to be present in each of the cluster cores. Although we have used reasonable estimates based on present evidence, they may in fact be somewhat low for ω Cen. The feature that *is* sensitive only to the observed difference in mass segregation between the two clusters is the ratio of the number of systems containing giants to the number of systems containing main-sequence stars, ($\sim 3\%$ for ω Cen and $\sim 15\%$ for 47 Tuc).

3.2. Luminosity-Period Distributions

The distributions plotted in figures 3 through 7, and described in this section, resulted from simulations in which ξ was set to 0.5 and j_{ej} was selected to be j_{wd}. That is, 50% of the mass in the "Roche shell" was assumed to be ejected from the system during capture and circularization, and the mass carried away with it a specific angular momentun appropriate to the the orbital motion of the white dwarf.

Figure 3 shows the distributions of *accretion* luminosity and orbital periods for systems that are undergoing mass transfer during the present epoch, for 47 Tuc (top panel) and ω Cen (bottom panel). Each dot or open circle represents a binary system. The number of points in each figure is roughly 100 times the number of active systems that would be present today, if the number of 1.1 $M_{\odot}$ white dwarfs present in the core of the clusters is $\sim$ 2500 for 47 Tuc and $\sim$ 25,000 for ω Cen (see §2.2 and §2.3). The accretion luminosity graphed in these figures is calculated from $L_{acc} = M\dot{M}G/R$, where $\dot{M}$ is the rate of mass transfer, M is the mass of the white dwarf, and R is its radius. Steady nuclear burning of the accreted matter on the surface of the white dwarf is not expected for the range of parameters encountered (see, e.g., Nomoto [1982, 1987]; Papaloizou, Pringle, & MacDonald [1982]; and Iben [1982]). Systems in which the white dwarf's companion is a main-sequence star are indicated with small dots (below the period gap) and open circles (above the period gap), while systems in which the white dwarf's companion is a giant are indicated with somewhat larger dots.

The most densely populated areas (small dots forming inverted "L" shaped regions) are those containing low-luminosity systems ($L_{acc} < 10^{33.2}$ ergs s^{-1}) with main-sequence companions. The orbital periods are in the range of $\sim$ 1 hr $< P_{orb} <$ 2.4 hr and these systems are in the post "period gap" phase (see §2.5.3). The open circles with $\sim 3 < P_{orb} < 5$ hours represent systems with main-sequence companions which have not yet entered the period gap. In plotting the systems containing main-sequence companions, we deliberately introduced a random smearing, by at most 30%, in L_{acc} in order (i) to introduce some realism (e.g., to simulate viewing the systems from different angles with respect to an obscuring accretion disk) and (ii) to decrease the density of plotted points so that the eye can better distinguish changes in density. Much less densely populated is the wide swath of higher luminosity systems which stretches from periods of $\sim$ 5 hours to $\sim$ 100 days, containing subgiant or giant companions. Relative to the number of low-luminosity systems which contain a main-sequence donor, there are many fewer such active giant donor systems in ω Cen than there are in 47 Tuc. The reason for this is that the greater degree of mass segregation in 47 Tuc increases the likelihood that a white dwarf and a giant will interact in the core of the cluster.

As described above, most of the systems containing main-sequence stars lie along three easily discernible tracks with an inverted "L" shape. These tracks correspond to the three

discrete mass classes (1.1, 0.75, and 0.6 $M_\odot$) that contain white dwarfs in Meylan's (1987, 1989) models of the 47 Tuc and ω Cen clusters. If we had used a more realistic continuous distribution of white dwarf masses, the three sets of tracks in Figure 3 would have blended together, but would still have occupied basically the same region of the $L_{acc} - P_{orb}$ plane.

The distributions shown in Figure 3 clearly reflect the information on binary evolution contained in Figure 2, especially with regard to the relative lifetimes of the different stages of mass transfer. Comparison with Figure 2 also gives a very clear impression of which systems contain main-sequence donors and which contain giants; in the latter case, an approximate core mass of the giant donor can be inferred. For systems containing main-sequence donor stars, the most heavily populated regions are those with the lowest luminosities ($L_{acc} < 10^{31.5}$ ergs s^{-1}) and hence the longest lifetimes and correspondingly greater probabilities of being present at the current epoch.

The calculated luminosity distributions for 47 Tuc and ω Cen are plotted in Figures 4 and 5, respectively. The results used to produce these figures were basically the same as for Figure 3 except that, in order to enhance the statistical accuracy, the numbers of white dwarfs followed were 1000 times the actual numbers expected in 47 Tuc and ω Cen, respectively. In panel (b) of Figures 4 and 5 is plotted the distribution of accretion luminosities ($L_{acc} = G\dot{M}M/R$) of systems undergoing mass transfer at the present epoch. These luminosities span the range from $\sim 10^{30.5}$ to 10^{35} ergs s^{-1}, though for ω Cen there are very few systems with $L_{acc} > 10^{33.5}$ ergs s^{-1} since very few of the donor stars are expected to be giants ($\sim$ 3% in ω Cen vs. $\sim$ 15% in 47 Tuc). Approximately 40% of all systems have very low luminosities ($< 10^{32}$) ergs s^{-1}; these are exclusively systems with main-sequence companions, below the orbital period gap and after the orbital period minimum (see §2.5.3). The somewhat spiky appearance of the distribution results from the fact that only a few discrete white dwarf masses were used in the simulations. The hatched histogram is simply a smoothed version of the actual distribution and should be closer to what the results would have been for a continuous distribution of white dwarf masses.

The luminosity distributions in panel (a) result from the same set of calculations, but here the accretion luminosities have been converted to X-ray luminosities ($\sim 0.5 - 4$ keV) using the prescription of Patterson & Raymond (1985). These authors have suggested that the apparent upper limit to the X-ray luminosity of *non-magnetic* CVs at $\sim 10^{32.5}$ ergs s^{-1} is a real physical effect related to the optical thickness of the boundary layer between the inner edge of the accretion disk and the surface of the accreting white dwarf (see also Pringle & Savonije 1979; Tylenda 1981; Narayan & Popham 1993). In addition to this "saturation" effect, the Patterson & Raymond (1985) prescription allows for only $\sim$ 10% of L_{acc} to emerge in the form of hard X-rays because of the emission geometry and the virial theorem.

In panels (c) and (d) of Figures 4 and 5 are plotted the integrated luminosities as a function of source luminosity. Note that, with the Patterson & Raymond (1985) prescription, ω Cen and 47 Tuc have integrated luminosities $L_x \sim 2-4 \times 10^{33}$ ergs s^{-1} while the corresponding values of L_{acc} are $1.5-2$ orders of magnitude larger. The observational implications of this difference will be pursued in §4.

The orbital period distributions of the simulated systems are shown for 47 Tuc and ω Cen in Figures 6 and 7, respectively. The distributions are shown separately for accretion luminosities $> 10^{31}$ and $> 10^{33}$ ergs s^{-1} in panel (b), and for X-ray luminosities (according to the Patterson & Raymond prescription discussed above) $> 10^{29}$ and $> 10^{31}$ ergs s^{-1} in panel (a). The main peak at orbital periods < 3 hours corresponds to systems with main-sequence companions below the "period gap", both before and after orbital period minimum (see §2.5.3). The relatively sharp falloff in systems with orbital periods above ~ 3 hours corresponds to the "period gap". The tail toward longer orbital periods ($8-300$ hours) is due to systems with giant or subgiant companions. As expected, the orbital period distributions for ω Cen show a relative dearth of systems with longer orbital periods because mass segregation is less pronounced in this cluster (Meylan 1987, 1989). The small fraction of systems with orbital periods exceeding ~ 5 days would, in principle, be susceptible to collisional disruption by other clusters stars (this limiting period applies to 47 Tuc, and would be even longer for ω Cen; see Rappaport, Putney, & Verbunt 1989 for details). However, the evolutionary lifetime of these wide systems is sufficiently short that this process will not substantially affect their population.

3.3. Scaling Our Results to Other Clusters

While our detailed simulations have been carried out for two specific globular clusters, the basic results can be extrapolated to other clusters by means of the appropriate scaling law. For two-body tidal captures, a proposed scaling law is given by

$$R \sim {\rho_c}^2 {r_c}^3 / v_{rms} \tag{3.1}$$

(Verbunt & Hut 1987; Verbunt, Lewin, & van Paradijs 1989), where R is the rate of capture of cluster stars, ρ_c is the density of stars in the core of the cluster, r_c is the core radius, and v_{rms} is the thermal speed of the cluster stars. This scaling law assumes that the number of cluster white dwarfs is proportional to the star density times the volume of the cluster core. We emphasize, however, that different scaling laws will apply for different capture mechanisms (see, e.g., Johnston, Kulkarni & Phinney 1992; Phinney & Kulkarni 1993).

A number of workers (Verbunt & Hut 1987; Verbunt et al. 1989; Bhattacharya & van den Heuvel 1991; Wijers 1991) have used scaling laws such as equation (3.1) to rank the rate of binary formation in all of the known globular clusters associated with the Galaxy. Such scalings indicate that (for two-body tidal capture) 47 Tuc and ω Cen should have

$\sim$ 4% and $\sim$ 1% of all of the binary formation in globulars, respectively. These values differ by relatively small factors ($\sim$ 25%) from those obtained by using a different scaling law due to Johnston et al. (1992; as reported by Wijers 1991). We can thus estimate that there should be between 5 and 15 $\times 10^3$ mass-transfer binaries containing white dwarfs in the Galactic globular cluster system. According to our luminosity distributions (see Figures 4 and 5) there should be $\sim$ 400 systems with X-ray luminosities above 10^{32} ergs s^{-1} (i.e., above the Rosat sensitivity threshold for moderate-to-long exposures). The expected numbers of mass transfer systems which have X-ray luminosities above various thresholds are summarized in Table 5. The observational consequences of these results are discussed in §4 below.

4. Predictions and Applications

Many of the systems in our simulations which are engaged in active mass transfer during the present epoch should have optical and X-ray properties similar to those of cataclysmic variables in the Galactic disk. Our results, presented in Tables 3 through 5 and Figures 4 through 7 are normalized to 2,500 and 25,000 white dwarfs of mass 1.1 $M_\odot$ in 47 Tuc and ω Cen, respectively. This corresponds to having set each of the normalization constants, $\mathcal{N}_{Tuc}$ and $\mathcal{N}_{Cen}$, introduced in §2.3, to unity. We find that there should be about 190 $\mathcal{N}_{Tuc}$ and 145 $\mathcal{N}_{Cen}$ active mass transfer binaries containing white dwarfs that were formed via two-body tidal capture. Almost all of the systems have X-ray luminosities lower than $10^{32.5}$ ergs s^{-1} because we have chosen to use a semi-empirical conversion from accretion luminosity to X-ray luminosity that is based on observations of CVs in the disk (see the discussion below and Patterson & Raymond 1985).

The systems that are generated in our simulations and are active at the present epoch are of three basic types. These are ordinary CVs with orbital period above the period minimum ($\sim$ 30%), systems which have evolved beyond the period minimum and which have mass transfer rates $< 3 \times 10^{-11} M_\odot$ yr^{-1} ($\sim$ 60%), and systems with giant donors ($\sim 3 - 15$%, depending on the cluster model). For the latter two classes of objects, the observational properties are difficult to predict in detail since these are not well studied in the nearby Galactic plane.

4.1 Applications to Optical Observations

There have been many attempts over the years to optically identify CVs in globular clusters. The obvious difficulties in making such identifications include the intrinsic faintness of the CVs in quiescence, and the crowded fields, especially near or within the cluster cores. Saywer-Hogg & Wehlau (1964) reported on three historical novae associated with the globular clusters M80, NGC 6553, and M14, although none of these objects has been unambiguously been identified with a binary system in the respective cluster. (See also Mayall 1949, Hogg 1973, Webbink 1980, and references therein.) There is a variable star

V101 in M5 that is a good candidate for a dwarf nova (Margon et al. 1981; Machin et al. 1990). Another candidate for a dwarf nova in M30 (V4) may turn out to be a foreground object (Margon & Downes 1983; Machin et al. 1990). Finally, there is a variable blue object (Auriére et al. 1989; Paresce et al. 1992) that may be associated with one of the low-luminosity X-ray sources in 47 Tuc (Hertz & Grindlay 1983a,b; Verbunt et al. 1993).

We begin here by briefly addressing the question of the expected rate of novae in globular clusters. It seems clear from the observational evidence (see above discussion) that there can not have been more than a relative handful of nova outbursts in globular clusters over the past century. At a peak outburst magnitude of $M_v \sim -5.5$ to -9.2, they should be very conspicuous, some even outshining their host cluster (median cluster magnitude $M_v \sim -7.2$ [Webbink 1985]), and therefore relatively easy to discover. Moreover, we infer from Hodge's (1992, and references therein) book on M31 that none of the more than 300 known novae in M31, has been associated with any of its more than 500 globular clusters. This paucity of observed novae in globular clusters provides a potentially powerful constraint on mechanisms, such as two-body tidal capture, that predict the presence of large numbers of CVs in globular clusters. We have therefore given careful consideration to the question of whether the predictions made here are contradicted by the small number of historical novae. To address this issue, we have included in our simulations and evolutionary studies, a calculation of the expected number of nova outbursts in 47 Tuc and ω Cen over the past century. For each system that is active, we store the probability that the white dwarf would have exhibited a nova outburst in the past 100 years. We took this probability to be just the ratio of the mass accreted in 100 years to the amount of mass necessary to trigger a nova outburst, given the mass accretion rate and the mass of the white dwarf in the particular system being followed (see, e.g., Nomoto 1982). These probabilities are summed and then normalized to the total number of accreting white dwarfs expected in a particular cluster. We conclude that there should have been about ~ 0.01 novae in each of ω Cen and 47 Tuc over the past century. When these rates are scaled to the Galactic globular cluster system as whole (see discussion below) we estimate that there should have been ~ 1 nova in globular clusters over the past century, consistent with the observations.

It is interesting to note that there are comments in the literature (e.g., Webbink 1980, Shara 1985) about the relative *overabundance* of novae in globular clusters. Shara's (1985) argument relating the observations of classical novae in globular clusters to the presence of a large population of "old novae" follows. Given that novae are thought to recur on timescales of $\sim 10^5 - 10^6$ years, and given that $2-3$ classical novae in globular clusters have been seen, it follows that (i) an "average" globular cluster may house as many as $10 - 100$ old novae, and (ii) it may be that there are $10 - 100$ times as many novae per capita in globular clusters as there are in the disk population (Shara 1985). These conclusions are consistent with the predictions presented here based on tidal capture.

Another possible conflict of optical observations with the prediction of large numbers of CVs in globulars is the apparent lack of detection of any outburst activity from the dwarf novae that should be present. The subset of the systems that emerge from our simulations which contains the largest number of candidates for dwarf novae have orbital periods below the period gap, but before minimum orbital period (see §2.5.3). These systems typically have mass transfer rates of between 3×10^{-11} and $3 \times 10^{-10} M_{\odot}$ yr^{-1}. The number of such binaries that we find for 47 Tuc (~ 45) and ω Cen (~ 30) are listed in the last column of Table 5. Of these, some fraction (e.g., perhaps 50%) might be dwarf novae, in particular U Gem-type objects. During outbursts, these sources have M_V in the range of +4 to +6. In globular clusters with distances in the range of $3 - 12$ kpc, the apparent visual magnitude would range from 16.5 to 21.5. CVs flaring to the lower of these values presumably should be detectable if the object is somewhat away from the center of the cluster. (In this regard, we note that $\sim 80\%$ of the tidal captures of interest to this work should occur within ~ 2 core radii [Verbunt & Meylan 1988].) Clearly, well defined upper limits on the numbers of such objects in globular clusters, produced either through the use of existing data bases or in future searches, have an important role to play.

However, the failure of most of the optical searches which have been performed to date, to identify large numbers of CVs in globular clusters, may serve to constrain production mechanisms. It is important to note though, that until recently, such searches have been hindered by the difficulty of resolving stars in the dense cores of globular clusters. This problem can be partially circumvented by the use of HST with its high resolution which, even now, is quite adequate to resolve individual stars at the cluster center (see, e.g., Margon et al. 1991; Paresce et al. 1991; and Paresce, de Marchi, & Ferraro 1992). For example, Shara (1993) studied approximately 1/4 of the core region of NGC 6752 with HST to search for CVs based on their temporal variability. He found no evidence for CVs with luminosity $> 10^{33}$ ergs s^{-1}. When we scale our results to NGC 6752 (with the use of eq. [3.1]) we predict that there should be $\sim 30 - 100$ CVs in this cluster, depending on whether we use the results from the ω Cen or 47 Tuc simulations, respectively; only $\sim 8 - 15$ of these are expected to have accretion luminosities $> 10^{33}$ ergs s^{-1}. However, with the Shara (1993) study, which was limited to $\sim 1/4$ of the core region of this cluster, one might expect to have detected fewer than 4 CVs; hence this observational study may not be at odds with the predictions made here.

4.2 Applications to X-Ray Observations

The first high-sensitivity survey of globular cluster X-ray sources was carried out with the Einstein observatory (Hertz & Grindlay 1983a,b). These observations of ~ 80 clusters yielded detections of 10 luminous ($10^{36} - 10^{38}$ ergs s^{-1}) X-ray sources (known from earlier studies) and 15 new lower-luminosity sources ($10^{32} - 10^{34.5}$ ergs s^{-1}) in 8 different clusters. Thus, the cluster sources seem to form two distinct classes with the more luminous

sources almost certainly containing accreting neutron stars in binary systems. All but two of the luminous systems exhibit the type of X-ray burst that has been associated with thermonuclear flashes on the surface of a weakly magnetized neutron star (e.g., Joss 1978; Lewin, van Paradijs, & Taam 1993). The lower luminosity sources have been hypothesized to be cataclysmic variables (Hertz & Grindlay 1983a) or perhaps neutron star binaries in a quiescent state (see, e.g., Verbunt et al. 1993).

More recent observations with Rosat have also added to the inventory of X-ray sources in globular clusters. The Rosat all-sky survey, which was sensitive to sources with luminosities as low as $10^{32.5}$ to 10^{35} ergs s^{-1}, depending on the cluster distance (Verbunt et al. 1993), led to the discovery of two luminous sources, in Ter 6 and in NGC 6652 (Predehl, Hasinger, & Verbunt 1991), as well as a supersoft X-ray source in NGC 5272 (M3; Verbunt et al. 1993, Hertz, Grindlay, & Bailyn 1993). As transients, the first two of these may bear on the question of whether the low-luminosity sources are low-mass X-ray binaries (LMXBs) in a quiescent state instead of an entirely different class of object. The supersoft source in NGC 5272 has a luminosity of $\sim 10^{35-36}$ ergs s^{-1} and a spectrum quite unlike that of other cluster sources. Therefore, while it is an intrinsically very interesting object, it may not be relevant to the nature of the low-luminosity cluster sources.

Pointed observations of 7 clusters with the PSPC instrument on Rosat (Johnston, Verbunt, & Hasinger 1993) have led to the discovery of sources in NGC 6341, 6397, 6656, 6752, and 7099, all in the range of $10^{32} - 10^{33}$ ergs s^{-1}. Moreover, Johnston et al. (1993) and Verbunt et al. (1993) report, based on Rosat observations, that (i) the Einstein source in 47 Tuc (Hertz & Grindlay 1983a,b) actually consists of 4 or more sources, and (ii) most of the 4 off-center low-luminosity sources in ω Cen (Hertz & Grindlay 1983a,b) are likely to be background or foreground objects, unrelated to ω Cen. Recently, Grindlay (1993) and Cool et al. (1993) made pointed Rosat HRI observations of NGC 6397 and NGC 6752 and report the discovery of at least 9 sources within 4 core radii of these clusters with luminosities in the range of $0.3 - 2 \times 10^{32}$ ergs s^{-1}. Finally, Rappaport et al. (1993) used the Rosat HRI to image 9 globular clusters with central densities in the range of $10^4 - 10^5 M_\odot$ pc^{-3} that had not previously been observed with the Einstein observatory. Sources were identified with two of the clusters: NGC 6304 and Pal 2, with luminosities of 1.2×10^{33} ergs s^{-1} and 1.1×10^{34} erg s^{-1}, respectively. These observational X-ray results are summarized in Table 6.

To our knowledge, none of the low-luminosity sources discussed above has yet been optically identified, with the possible exception of the CV-like object discovered near the 47 Tuc sources (Auriére et al. 1989; Paresce et al. 1992).

In all, there are now approximately 25 low-luminosity globular cluster sources known. Speculation as to their nature centers around an association with cataclysmic variables (Hertz & Grindlay 1983a) or with LMXBs in quiescence (however, see Bailyn, Grindlay,

& Garcia 1990 and Verbunt et al. 1993 for an alternative suggestion that some may be conglomerates of large numbers of RS CVn-type stars). Not enough is known empirically or theoretically about transient LMXBs, in particular about their intensities and X-ray spectra, to allow for a quantitative evaluation of the quiescent LMXB hypothesis. With the results presented here, however, one can directly evaluate the hypothesis that the low-luminosity cluster sources are cataclysmic variables.

Empirical evidence in this regard can be found in Cordova & Mason's (1983) and in Patterson & Raymond's (1985) tabulation of the ~ 50 known cataclysmic variables in the galactic plane that have been detected in X-rays and have known distances, so that their luminosities can be estimated. The 1-10 keV luminosities of the *non-magnetic* CVs range from $\sim 10^{30}$ to $10^{32.5}$ ergs s^{-1}, with 80% of the sources below 10^{32} ergs s^{-1}. As discussed above, Patterson & Raymond (1985) have suggested that the apparent upper limit to the hard X-ray luminosity at $\sim 10^{32.5}$ ergs s^{-1} is a real physical effect. It is due to the optical thickness of the boundary layer between the inner edge of the accretion disk and the surface of the accreting white dwarf at high accretion rates. Recent theoretical work (see Narayan & Popham 1993 and the discussion in §3) lends support to this hypothesis. Moreover, the hard X-ray fluxes of the *magnetic* CVs (DQ Her and AM Her systems) are no higher than $\sim 10^{33}$ ergs s^{-1} (Norton & Watson 1989; Chanmugam, Ray, & Singh 1991). We note that 7 magnetic CVs (AM Her systems) do have soft X-ray (< 0.3 keV) luminosities in the range of $\sim 10^{32.5}$ to $10^{34.5}$ ergs s^{-1} (Patterson 1984; Watson 1986; Cropper 1990; Chanmugam et al. 1991). However, no source with such a soft X-ray component has been reported for any of the globular cluster sources listed in Table 6 (for several of the clusters the substantial hydrogen column densities in their direction would absorb much of the soft X radiation). Therefore, it seems evident that a number (fewer than half) of the known low-luminosity cluster sources are one to two orders of magnitude more luminous (in the 1-5 keV band) than the most luminous galactic plane CVs tabulated by Cordova & Mason (1983), Patterson & Raymond (1985), and Chanmugam et al. (1991). Finally in this regard we note that, given the sensitivities of the deepest Einstein and Rosat obervations of globular clusters ($\sim 10^{32}$ ergs s^{-1}), most of the cataloged CVs would not have been detected at typical globular cluster distances.

Therefore, we tentatively conclude that the ~ 5 low-luminosity sources with $L_x > 10^{33}$ ergs s^{-1}, listed in Table 6, as well as the 4 sources in 47 Tuc, are not CVs of the type observed in the galactic plane. It is possible, of course, that if CVs are produced in great numbers in globular clusters via two-body tidal capture (see, e.g., Verbunt & Meylan 1988; Romani 1990; Chanmugam et al. 1991; Rappaport & Di Stefano 1993), perhaps a modest fraction have properties that are very different from those of CVs in the solar neighborhood. For example, the distribution and orientation of white dwarf magnetic fields could be substantially different from those of the local population of CVs (Chanmugam et

al. 1991) which are presumably dominated by systems which have evolved from primordial binaries.

We now directly compare the observational facts concerning X-ray sources in globular clusters with the calculations in this work. As discussed above, there are about 25 low-luminosity globular cluster X-ray sources, about 40% of which have X-ray luminosities $L_x > 10^{33}$ ergs s^{-1} (see Table 6). If, in contrast to CVs in the Galactic disk, a substantial fraction of all the accretion luminosity came out in X-rays, our calculations would predict ~ 45 and 20 such X-ray sources in 47 Tuc and ω Cen, respectively, and ~ 1500 sources in all of the Galactic globular clusters. This is more than sufficient to explain all the globular clusters sources with $L_x > 10^{33}$ ergs s^{-1} that have been observed to date. On the other hand, with the Patterson & Raymond (1985) prescription for converting L_{acc} to L_x very few, if any, sources would be expected with $L_x > 10^{33}$ ergs s^{-1}. This distinction is crucial to our understanding of the more luminous of the low-luminosity cluster sources.

Our calculations can also be used to test the viability of the Patterson & Raymond (1985) prescription in the globular cluster context. This test involves the calculated X-ray luminosity integrated over all the CVs in a particular cluster. Basically, we show here that if the X-ray luminosity is a substantial fraction of the accretion luminosity (especially for $L_{acc} > 10^{33}$ ergs s^{-1}) the expected integrated cluster X-ray luminosities would be significantly greater than those observed. For this test, we utilize a uniform set of limits on X-ray luminosity for 21 clusters obtained with the Einstein IPC (Hertz & Grindlay 1983b). These clusters, with the corresponding limits for point X-ray source detection (in the 0.5 - 4.5 keV band), are listed in Table 7; only clusters with upper limits of $< 10^{33.5}$ ergs s^{-1} were included. We note that the clusters ω Cen and 47 Tuc happen not to be ideal clusters with which to check the integrated luminosities against the model calculations. In the case of 47 Tuc, there are at least 4 discrete sources in the core (Verbunt et al. 1993), each of which (if there are only 4 sources) is above the luminosity of typical Galactic plane CVs (see the above discussion). The core of ω Cen has such a large angular extent that the Einstein IPC point response function (see below) covers only a small fraction of the core. Nonetheless, we show later that the available information for these two clusters is consistent with the computed integrated X-ray luminosities of CVs if the Patterson & Raymond (1985) prescription for converting L_{acc} to L_x is utilized.

Conveniently, the limits on *point sources* given in Table 7 can also be converted to limits on the *integrated cluster luminosity* with only a couple of reasonable assumptions. The IPC point response function (PRF) can be represented by a two-dimensional Gaussian with σ having values between 0.5′ and 0.7′ over the energy range 1-10 keV (Seward 1993). This is comparable to the angular size of the cores of many globular clusters and, therefore, the limiting luminosity for a point source is closely related to the limit on the integrated luminosity for all the sources in the cluster. We utilized an *ad hoc*, but plausible function

for how CVs might be distributed radially in a globular cluster. We then integrated this distribution against the two-dimensional Gaussian PRF to determine what fraction, F_L, of the integrated cluster luminosity would be found within the IPC-PRF. (We also tested a range of different functions for the radial distribution of CVs within a cluster, and found that our results were not highly sensitive to the uncertainties in this function.) The value of F_L was multiplied by the calculated integrated X-ray luminosity for that particular cluster to predict the signal within the IPC-PRF. (A better method for setting a limit on the integrated cluster X-ray luminosity would be to reanalyze the original IPC data to directly obtain a limit on extended sources, but this is beyond the scope of the present paper.)

To predict, based on our calculations, the expected integrated X-ray luminosities of the clusters listed in Table 7, we must scale our results for 47 Tuc and ω Cen to these clusters. To be certain that our particular choice of scaling law did not bias our results too strongly, we employed four rather different scaling laws, two of them somewhat *ad hoc*. The first scaling law was the one given by equation (3.1) which is appropriate for two-body tidal capture. The second is of the form

$$R \sim {\rho_c}^{0.5} M_c, \tag{4.1}$$

where M_c is the mass of the cluster core (Johnston et al. 1992); this semi-empirical law takes into account other types of capture processes, especially in the lower-density clusters. For the other two scaling laws, we simply used the total mass of the cluster and a concentration factor defined as r_t/r_c, the ratio of cluster tidal radius to core radius. (For post-core-collapse clusters we did not attempt to compute the latter scaling.) The values for the cluster parameters used in computing the scaling relations were taken from Webbink (1985) and Chernoff & Djorgovski (1989).

For each cluster in Table 7 we scaled our simulation results for both 47 Tuc and ω Cen, using all four scaling laws, to predict the integrated X-ray luminosity. In all cases we used the Patterson & Raymond (1985) prescription for converting L_{acc} to L_x. These expected scaled integrated luminosities, multiplied by the factor F_L (see above), are given in the 8 columns of Table 7 immediately following the Einstein upper limit. Note that, with the exception of a few individual entries (5 out of 160), all of the predicted integrated luminosities fall below the observational upper limits. When we used the same scaling laws, but made the assumption that L_x is a substantial fraction of L_{acc} (i.e., give up the Patterson & Raymond conversion) we found that more than half of the predicted integrated luminosities exceed the observed upper limits (some by more than an order of magnitude). Thus, we conclude that if there are anywhere near the number of CVs that we compute in globular clusters, the Patterson & Raymond (1985) prescription for converting L_{acc} to L_x (or one that has the same net effect of limiting L_x regardless of how large $\dot{M}$ is) is essential

in order that the expected integrated cluster X-ray luminosities not exceed already existing limits.

Finally, we return to the question of how the calculated integrated X-ray luminosites of ω Cen and 47 Tuc compare with the limits that can be set from the observations. Using the same type of analysis as discussed above, our calculations indicate that the Einstein IPC should have detected an integrated luminosity within its PRF of 10^{32} ergs s^{-1} and $10^{33.4}$ ergs s^{-1} from ω Cen and 47 Tuc, respectively. Here we have again made use of the Patterson & Raymond (1985) conversion factor. For ω Cen, where the IPC-PRF covers much less than the core radius, this luminosity is just below the detectability threshold. In the case of 47 Tuc, where the PRF is comparable in angular extent to that of the core radius, the predicted signal from the integrated luminosity is about a factor of 2 smaller than the signal from each of the point sources located near the center of this cluster. We also note that diffuse X-ray emission from over a $\sim 10' \times 10'$ region in each of these clusters has been reported by Hartwick, Cowley, & Grindlay 1982. The total luminosity associated with this emission is $\sim 8 \times 10^{32}$ and $\sim 3 \times 10^{33}$ for 47 Tuc and ω Cen, respectively. Our present calculations do not address such diffuse emission.

5. Conclusions

In summary, we have used the calculations presented in this work to reach the following conclusions:

1. The mechanism of two-body tidal capture coupled with detailed consideration of binary evolution, leads to an unambiguous prediction of a large number of cataclysmic variables in globular clusters. These numbers are stable over a range of assumptions about the processes of capture and circularization, which are poorly understood at the present time. They are roughly an order of magnitude larger than previous predictions which have not included evolution calculations. We note that our binary *production rates* are in reasonable agreement with those of previous studies (Verbunt and Meylan [1988] and Davies [1992]). However, we have done detailed evolution calculations that indicate that a large number of the *mass transfer systems* are long-lived, capable of remaining active for essentially a Hubble time. If observations can conclusively rule out a substantial population of CVs in globular clusters, then, given the robustness of the predictions with respect to various assumptions about the capture/circularization process, the two-body tidal capture scenario will be seriously, perhaps fatally, damaged.
2. We have performed several checks that the large number of systems we predict is not ruled out by the paucity of CVs that have been discovered by observations to date. In particular, the number of nova explosions that might have occurred during the past century is compatible with (or even slighly smaller than) the number of recorded novae. Moreover, at least at the present time, our calculations of the numbers and

luminosities of CVs are not obviously at odds with the lack of optical detection of numerous dwarf novae in globular clusters, but this needs to be quantified further.

3. The predicted integrated globular cluster X-ray luminosities will be consistent with existing observational upper limits only if the X-ray luminosity of individual systems is substantially less than the accretion luminosity (as appears to be the case for the well-studied CV population nearby in the Galactic disk). The Patterson & Raymond (1985) prescription for converting L_{acc} to L_x works very well in this regard. If observational limits on the integrated cluster luminosities can be pushed down another factor of ~ 5, then the two-body tidal formation scenario would begin to be seriously constrained. If the Patterson & Raymond prescription holds, then our calculations provide no explanation for globular cluster X-ray sources with $L_x > 10^{33}$ ergs s^{-1}. Our simulations do, however, still account for all of the sources observed at lower luminosities.
4. The conclusion above may be turned around as follows. If the efficiency of two-body tidal capture is not dramatically smaller than the efficiency associated with even the most pessimistic mass stripping scenario that we have considered for the process of capture and circularization, then our results provide strong evidence that the majority of CVs in globular clusters do indeed behave similarly to CVs in the disk. In particular, when $\dot{M}$ is high, hard X-ray emission is greatly suppressed by an optically thick boundary layer where it is produced (see, e.g., Patterson & Raymond 1985).
5. Three-body and four-body interactions may be expected to enhance the numbers of CVs predicted here.
6. This is a time of active observational study of globular clusters across a broad spectrum of wavelengths. Recent observations, especially of low-luminosity X-ray sources, may be finding evidence of CVs in globular clusters. If so, then the predictions derived in this work indicate that several times as many sources should be found when the limits on L_x are pushed down to 10^{31} ergs s^{-1}. It is therefore possible that recent and current observations are just beginning to see the proverbial tip of the CV population "iceberg".

We thank M. Metzger for pointing out the importance of the integrated cluster X-ray luminosities; A. Cool for detailed discussions on the status of observational data; and C. Bailyn, M. Krockenberger, B. Margon, K. Nomoto, and M. Shara for helpful discussions. One of us (RD) would like to thank the Aspen Center for Physics for its hospitality during the time this manuscript was being prepared. This work was supported in part by the National Aeronautics and Space Administration under grants NAGW-1545 and NAG5-1983, and by the Science Scholars Fellowship Program at the Bunting Institute under a grant from the Office for Naval Research.

REFERENCES

Auriére, M., Koch-Miramond, L., & Ortolani, S. 1989, A&A, 214, 113.

Bailyn, C.D., Grindlay, J.E., and Garcia, M.R. 1990, ApJ, 357, L35.

Bailyn, C.D., & Grindlay, J.E. 1990, ApJ, 353, 159.

Bailyn, C.D. 1988, *Nature*, **332**, 330.

Bhattacharya, D., & van den Heuvel, E.P.J. 1991, Physics Reports, 203, 1.

Chanmugam, G., Ray, A. & Singh, K.P. 1991, ApJ, 375, 600.

Chernoff, D.F. & Djorgovski, G. 1989, ApJ, 339, 904.

Cool, A.M., Grindlay, J.E., Krockenberger, M., & Bailyn, C.D. 1993, ApJ, in press.

Cordova, F., & Mason, K.O. 1983, in Accretion Driven Stellar X-Ray Sources, eds. W.H.G. Lewin and E.P.J. van den Heuvel (Cambridge: Cambridge University Press), p.147.

Cropper, M. 1990, Space Sci. Rev., 54, 195.

Davies, M.B., Benz, W., and Hills, J.G. 1991, ApJ, 381, 449.

Davies, M.B., Benz, W., and Hills, J.G. 1992, ApJ, 401, 246.

Davies, M.B., Benz, W., and Hills, J.G. 1993, ApJ, in press.

Davies, M.B. 1992, Ph.D. thesis, Harvard University.

Di Stefano, R., and Rappaport, S. 1992, ApJ, 396, 587 (DR).

Fabian, A.C., Pringle, J.E., and Rees, M.J. 1975, MNRAS, 172, 15P.

Greiner, J., Hasinger, G., & Kahabka, P. 1991, A&A, 246, L17.

Grindlay, J.E. 1992, to be published in "Dynamics of Globular Clusters, ed. S. Djorgovski and G. Meylan, ASP Conference Series.

Hameury, J.M., King, A.R., Lasota, J.P., & Ritter, H. 1988, MNRAS, 231, 535.

Hameury, J.M., King, A.R., & Lasota, J.P. 1986, A&A, 162, 71.

Harpaz, A., & Rappaport, S. 1991, ApJ, 383, 739.

Hartwick, F.D.A., Cowley, A.P., & Grindlay, J.E. 1982, ApJ, 254, L11.

Hertz, P. & Grindlay, J.E. 1983a, ApJ, 267, L83.

Hertz, P. and Grindlay, J.E. 1983b, ApJ, 275, 105.

Hertz, P. & Grindlay, J.E., & Bailyn, C.D. 1993, ApJ, 410, L87.

Hodge, P. 1992, The Andromeda Galaxy (Dordrecht: Kluwer).

Hogg, H.S. 1973, Publ. David Dunlap Obs., 3, No. 6.

Hut, P., et al. 1992, PASP, 104, 981.

Iben, I. Jr. 1982, ApJ, 259, 244.

Iben, I. Jr. & Tutukoz, A.V. 1984, ApJ, 284, 719.

Johnston, H.M., Kulkarni, S.R., & Phinney, E.S. 1992, in X-Ray Binaries and Recycled Pulsars, ed. E.P.J. van den Heuvel & S. Rappaport (Dordrecht: Kluwer), p. 349.

Johnston, H.M., Verbunt, F., & Hasinger, G.R. 1993, A&A, in preparation.
Joss, P.C. 1978, ApJ, 225, L123.
Joss, P.C., & Rappaport, S. 1983, Nature, 304, 419.
Joss, P.C., Rappaport, S., & Lewis, W. 1987, ApJ, 319, 180.
Kochanek, C.S. 1992, ApJ, 385, 604.
Kulkarni, S.R. & Narayan, R. 1988, ApJ, 355, 755.
Kulkarni, S.R., Narayan, R., and Romani, R.W. 1990, ApJ, 356, 174.
Lee, H.M. & Ostriker, J.P. 1986, ApJ, 310, 176.
Leonard, P.J.T. 1989, AJ, **98**, 217.
Lewin, W.H.G., van Paradijs, J., & Taam, R. 1993, Space Sci. Rev., in press.
Long, K.S., Helfand, D.J., & Grabelsky, D.A. 1981, ApJ, 248, 925.
Machin, G., Callanan, P.J., Charles, P., & Naylor, T. 1990, in Accretion Powered Compact Binaries, ed. C.W. Mauche (Cambridge University Press), p. 163.
Margon, B., Downes, R.A., & Gunn, J.E. 1981, ApJ, 247, L89.
Margon, B., & Downes, R.A. 1983, ApJ, 274, L31.
Margon, B. and Bolte, M. 1987, ApJ, 321, L61.
Margon, B., Anderson, S.F., Downes, R.A., Bohlin, R.C., & Jakobsen, P. 1991 Ap.J.Lett. 369, L71.
Mayall, M.W. 1949, AJ, 54, 191.
McMillan, S.L., McDermott, P.N., & Taam, R.E. 1987, ApJ, 318, 261.
Meylan, G. 1987, A&A, 184, 144.
Meylan, G. 1989, A&A, 214, 106.
Narayan, R. & Popham, R. 1993, CfA preprint.
Nomoto, K. 1982, ApJ, 253, 798.
Nomoto, K. 1987, in "The Origin anf Evolution of Neutron Stars", ed. D.J. Helfand, and J.H. Huang (Dordrecht: Reidel), p 281.
Nomoto, K., Nariai, K., & Sugimoto, D. 1979, PASJ, 31, 287.
Norton, A.J., & Watson, M.G. 1989, MNRAS, 237, 715.
Papaloizou, J.C.B., Pringle, J.E., & MacDonald, J. 1982, MNRS, 198, 215.
Patterson, J. 1984, ApJS, 54, 443.
Patterson, J. & Raymond, J.C. 1985, ApJ, 292, 535.
Paresce, F., De Marchi, G., & Ferraro, F.R. 1992, Nature, 360, 46.
Phinney, E.S. and Kulkarni, S.R. 1993, Nature, in press.
Podsiadlowski, Ph. 1991, Nature, 350, 136.
Predehl, P., Hasinger, G., & Verbunt, F. 1991, A&A, 246, L21.
Press, W.H., & Teukolsky, S.A. 1977, ApJ, 213, 183.

Pringle, J.E. & Savonije, G.J. 1979, MNRAS, 187, 777.

Pylyser, E.H.P., Savonije, G.J. 1988, A&A, 191, 57.

Pylyser, E.H.P., Savonije, G.J. 1989, A&A, 208, 52.

Rappaport, S.A., Joss, P.C., and Webbink R.F. 1982, ApJ, 252, 616.

Rappaport, S, Verbunt, F., & Joss, P.C. 1983, ApJ, 275, 713 (RVJ).

Rappaport, S., & Joss, P.C 1984, ApJ, 283, 232 (RJ).

Rappaport, S., Nelson, L.A., Ma, C.P., & Joss P.C. 1987, ApJ, 322, 842.

Rappaport, S.A., Putney, A., and Verbunt, F. 1989, ApJ, 345, 210.

Rappaport, S. & Di Stefano, R. 1993, to appear in Proceedings of the 2nd Technion Haifa Conference on Cataclysmic Variables and Related Objects, Eilat, Israel, January 1993, eds. O. Regev and G. Shaviv.

Rappaport, S., Dewey, D., Levine, A., & Macri, L. 1993, submitted to ApJ.

Rasio, F.A., and Shapiro, S.L. 1990, ApJ, 354, 201.

Rasio, F.A., and Shapiro, S.L. 1991, ApJ, 377, 559.

Ray, A., Kembhavi, A.K., & Antia, H.M. 1987, A&A, 184, 164.

Romani, R.W. 1990, ApJ, 357, 493.

W.H.G. Lewin & E.P.J. van den Heuvel (Cambridge: Cambridge University Press), p. 343.

Sawyer-Hogg, H., & Wehlau, A. 1964, J. Roy. Astr. Soc. Canada, 58, 163.

Seward, F. 1993, private communication.

Shara, M. 1993, private communication.

Spruit, H.C. & Ritter, H. 1983, A&A, 124, 267.

Tylenda, R. 1981, Acta. Astr., 31, 127.

Truemper, J., et al. 1991, Nature, 349, 579.

van den Heuvel, E.P.J., Bhattacharya, D., Nomoto, K., & Rappaport, S.A. 1992, A&A, 262, 97.

Verbunt, F., Lewin, W.G.H., & van Paradijs, J. 1989, MNRAS, 241, 51.

Verbunt, F., Hasinger, G., Johnston, H.M., & Bunk, W. 1993, preprint from the Sterrekundig Instituut of Utrecht.

Verbunt, F., & Hut, P. 1987, in The Origin and Evolution of Neutron Stars, eds. D.J. Helfand and J.H. Huang, (Dordrecht: Reidel), p. 187.

Verbunt, F., & Meylan, G. 1988, A&A, 203, 297.

Watson, M.G. 1986, in The Physics of Accretion Onto Compact Objects, ed. K.O. Mason, M.G. Watson, & N.E. White (Berlin: Springer-Verlag), p.97.

Webbink, R.F. 1980, in Close Binary Stars: Observations and Interpretation, eds. M.J. Plavec, D.M. Popper, & R.K. Ulrich, (Dordrecht: Reidel), p 561.

Webbink, R.F., Rappaport, S, & Savonije, G.J. 1983, ApJ, 678, 693 (WRS).

Webbink, R.F. 1985, in Dynamics of Star Clusters, eds. J. Goodman and P. Hut, p. 541.
Wijers, R. 1992, private communication.

Table 1

Tidal Capture Events in 47 Tuc					
Captured Stars	*M* *White Dwarf Mass*	*R* *Rate (per white dwarf per second)* [1]	ρ *Relative Number of White Dwarfs in Core*	[2] *Average Cluster Factor*	*N* *Number of Captures* [3] *(per* 15×10^9 *yrs) Scaled to 2500* $1.1 M_\odot$ *White Dwarfs*
Giants	1.1	2.6×10^{-19}	1.0	1.4	430
	0.75	1.6×10^{-19}	0.8	1.8	272
	0.6	1.5×10^{-19}	1.3	2.0	461
Total Number of Giants Captured					**1024**
Main Sequence Stars	1.1	5.7×10^{-20}	1.0	1.6	108
	0.75	3.3×10^{-20}	0.8	2.4	75
	0.6	3.0×10^{-20}	1.3	2.8	129
Total Number of Main Sequence Stars Captured					**312**

[1] Rate of tidal capture (with collisions included as a subset of tidal capture) in the core of the cluster.

[2] The average cluster factor is the enhancement factor that yields the total number of each type of event in the cluster as a whole, given the number of such events that occur within the core. Mathematically, it is $1/\langle f(m, M)\rangle_m$, where M represents the mass of the white dwarf, and the average is taken over m, the mass of the captured star, and $f(m, M)$ is the fraction of captures of extended stars of mass m by compact stars of mass M that occur in within one core radius of the center of the cluster.

[3] These calculations have assumed that there are 2500 $1.1 M_\odot$ white dwarfs in the core of the cluster. The number of white dwarfs in the core for each of the other two mass classes is obtained by multiplying by the factor ρ (column 4). The numbers of events (N) listed in column 6 are the *total* for the cluster.

Table 2

Tidal Capture Events in ω Cen					
Captured Stars	*M* *White Dwarf Mass*	*R* *Rate (per white dwarf per second)* [1]	ρ *Relative Number of White Dwarfs in Core*	[2] *Average Cluster Factor*	*N* *Number of Captures* [3] *(per* 15×10^9 *yrs) Scaled to 25,000* $1.1 M_\odot$ *White Dwarfs*
Giants	1.1	2.8×10^{-21}	1.0	1.6	53
	0.75	2.0×10^{-21}	0.7	2.0	34
	0.6	1.7×10^{-21}	1.1	2.2	50
Total Number of Giants Captured					**137**
Main Sequence Stars	1.1	5.0×10^{-21}	1.0	1.9	112
	0.75	2.8×10^{-21}	0.7	2.5	58
	0.6	2.7×10^{-21}	1.1	2.8	98
Total Number of Main Sequence Stars Captured					**268**

[1] Rate of tidal capture (with collisions included as a subset of tidal capture) in the core of the cluster.

[2] The average cluster factor is the enhancement factor that yields the total number of each type of event in the cluster as a whole, given the number of such events that occur within the core. Mathematically, it is $1/\langle f(m, M)\rangle_m$, where M represents the mass of the white dwarf, and the average is taken over m, the mass of the captured star, and $f(m, M)$ is the fraction of captures of extended stars of mass m by compact stars of mass M that occur in within one core radius of the center of the cluster.

[3] These calculations have assumed that there are 25,000 $1.1 M_\odot$ white dwarfs in the core of the cluster. The number of white dwarfs in the core for each of the other two mass classes is obtained by multiplying by the factor ρ (column 4). The numbers of events (N) listed in column 6 are the *total* for the cluster.

Table 3

Number of Systems in 47 Tuc *Scaled to 2500 $1.1M_\odot$ white dwarfs in the cluster core*						
Parameters Mass Loss ξ (1)	Angular Momentum j_{ej} (2)	Type of Star Captured	Number of Capture Events (3)	Collisions and Catastrophic Interactions (4)	Mass Transfer begins before present epoch (5)	Mass Transfer during present epoch (6)
0.0	0	main seq. giants	305 1129	155 715	145 410	128 27
		Total	**1434**	**870**	**555**	**150**
0.5	0	main seq. giants	305 1129	105 532	182 590	166 31
		Total	**1434**	**637**	**772**	**197**
0.5	j_{wd}	main seq. giants	305 1129	105 543	179 579	164 30
		Total	**1434**	**648**	**758**	**194**
0.5	j_{ex}	main seq. giants	305 1129	107 685	192 438	176 23
		Total	**1434**	**792**	**630**	**199**
1.0	0	main seq. giants	305 1129	112 519	132 588	119 27
		Total	**1434**	**631**	**720**	**146**
1.0	j_{wd}	main seq. giants	305 1129	112 519	132 589	119 27
		Total	**1434**	**631**	**721**	**146**
1.0	j_{ex}	main seq. giants	305 1129	112 656	172 467	159 25
		Total	**1434**	**768**	**639**	**184**

(1) Percentage of the "Roche shell" stripped from the target during circularization (see §2).
(2) Specific angular momentum of mass that is ejected from the system during capture and circularization.
(3) Collisions are included as a subset of capture events.
(4) The category of "collisions and catastrophic interactions" consists of: direct collisions; interactions in which the stars do not physically touch on the first pass, but in which there is so much mass stripped from the extended star that its mass after the interaction is likely to be less than $\sim 0.08M_\odot$; and interactions in which the distance of closest approach was such that, even after circularization, the extended star was still over-filling its Roche lobe.
(5) Mass transfer occurs when the extended star fills its Roche lobe. For main-sequence stars this can occur through a decrease in the orbital separation due to a dissipative process—either magnetic braking or gravitational radiation. For giants, the expansion of the giant may also allow the star to overfill its Roche lobe.
(6) Mass transfer continues in the present epoch. These systems may be observable as cataclysmic variables.

Table 4

Number of Systems in ω Cen *Scaled to 25000* $1.1M_{\odot}$ *white dwarfs in the cluster core*						
Parameters Mass Loss ξ (1)	Angular Momentum j_{ej} (2)	Type of Star Captured	Number of Capture Events (3)	Collisions and Catastrophic Interactions (4)	Mass Transfer begins before present epoch (5)	Mass Transfer during present epoch (6)
0.0	0	main seq. giants	270 138	137 88	123 49	118 3
		Total	**408**	**225**	**172**	**121**
0.5	0	main seq. giants	270 138	88 68	151 69	147 4
		Total	**408**	**156**	**220**	**151**
0.5	j_{wd}	main seq. giants	270 138	88 70	148 68	143 4
		Total	**408**	**158**	**216**	**147**
0.5	j_{ex}	main seq. giants	270 138	92 85	167 52	162 3
		Total	**408**	**177**	**219**	**165**
1.0	0	main seq. giants	270 138	112 65	91 71	87 4
		Total	**408**	**177**	**162**	**91**
1.0	j_{wd}	main seq. giants	270 138	112 65	90 71	86 4
		Total	**408**	**177**	**161**	**90**
1.0	j_{ex}	main seq. giants	270 138	112 82	138 55	134 3
		Total	**408**	**194**	**193**	**137**

(1) Percentage of the "Roche shell" stripped from the target during circularization (see §2).
(2) Specific angular momentum of mass that is ejected from the system during capture and circularization.
(3) Collisions are included as a subset of capture events.
(4) The category of "collisions and catastrophic interactions" consists of: direct collisions; interactions in which the stars do not physically touch on the first pass, but in which there is so much mass stripped from the extended star that its mass after the interaction is likely to be less than $\sim 0.08M_{\odot}$; and interactions in which the distance of closest approach was such that, even after circularization, the extended star was still over-filling its Roche lobe.
(5) Mass transfer occurs when the extended star fills its Roche lobe. For main-sequence stars this can occur through a decrease in the orbital separation due to a dissipative process—either magnetic braking or gravitational radiation. For giants, the expansion of the giant may also allow the star to overfill its Roche lobe.
(6) Mass transfer continues in the present epoch. These systems may be observable as cataclysmic variables.

Table 5

Numbers of Active Mass Transfer Binaries(1)				
	$L_x > 10^{29}$	$L_x > 10^{31}$	$L_x > 10^{32}$	$10^{32.2} < L_{acc} < 10^{33.2}$
ω Cen	145	60	4	30
47 Tuc	190	90	20	45
All Clusters(2)	15,000	6,000	450	3,000
All Clusters(3)	4,500	2,000	430	1,000

(1) Calculated numbers of active mass-transfer CV binaries (columns 1 – 3) with X-ray luminosity (computed with the Patterson & Raymond [1985] prescription for converting from L_{acc} to L_x) above the values indicated at the top of the column; and (column 4) with accretion luminosity in the range typical of CVs below the period gap but above minimum orbital period. All luminosities are expressed in ergs s^{-1}. The results are for the model with $\xi = 0.5$ and $j_{ej} = j_{wd}$ (see Tables 3 and 4, and §2.4), and assumed white dwarf populations of 2,500 and 25,000 in the cores of 47 Tuc and ω Cen, respectively.

(2) Scaled from the ω Cen results

(3) Scaled from the 47 Tuc results

Table 6

Low-Luminosity X-Ray Sources in Globular Clusters				
Cluster	Popular Name	Number of Sources	L_x	Reference(1)
NGC 104	47 Tuc	4	33.6 (2)	HG83; V93
Pal 2		1	34.5	R93
NGC 1904	M79	1	33.6	HG83
NGC 5139	ω Cen	1 (?)	32.6	HG83; V93; J93
NGC 5272	M3	1	33.6	HG83
NGC 5824		1	34.0	HG83
NGC 6304		1	33.5	R93
NGC 6341	M92	1	32.3	V93; J93
NGC 6397		5	31.5-32	G93; C93
NGC 6541		1	33.0	HG83
NGC 6656	M22	3	32-32.5	HG83; V93
NGC 6752		4	31.8-32.5	G93; C93
NGC 7099	M30	1	32.1	V93; J93

(1) References:

HG83 — Hertz & Grindlay (1983a,b)
V93 — Verbunt et al. (1993)
R93 — Rappaport et al. (1993)
G93 — Grindlay (1993)
C93 — Cool et al. (1993)
J93 — Johnston, Verbunt, & Hasinger (1993)

(2) Each of the 4 sources is taken to have 1/4 of the total X-ray luminosity inferred from the Einstein HRI and IPC measurements of $\sim 10^{34.2}$ erg s^{-1}.

Table 7

Limits on the Integrated X-Ray Luminosities of Selected Clusters(1)									
		47 Tuc				ω Cen			
Cluster	L_{IPC}(2)	V(3)	P(4)	M_T(5)	C(6)	V(3)	P(4)	M_T(5)	C(6)
NGC 4590	33.5	31.1	31.7	32.4	32.9	31.5	31.2	31.9	32.9
NGC 5904	33.5	32.6	32.8	33.3	32.8	33.0	32.4	32.8	32.8
NGC 6171	33.4	31.4	31.8	32.3	32.8	31.8	31.4	31.9	32.8
NGC 6218	33.3	31.4	31.9	32.4	32.7	31.8	31.4	31.9	32.7
NGC 6254	33.1	31.9	32.1	32.6	32.8	32.3	31.7	32.2	32.8
NGC 6333	33.5	32.5	32.7	32.8	33.0	32.9	32.3	32.4	33.0
NGC 6352	33.2	31.1	31.5	32.2	32.3	31.5	31.0	31.8	32.4
NGC 6366	32.8	30.1	30.8	30.8	32.1	30.5	30.3	30.4	32.1
NGC 6402	33.5	32.3	32.9	33.3	32.8	32.7	32.4	32.9	32.8
Pal 6	32.6	31.9	32.2	32.1	32.3	32.3	31.8	31.7	32.3
NGC 6517	33.3	33.2	32.8	32.7	—	33.7	32.3	32.3	—
NGC 6522	33.3	33.1	32.9	32.8	—	33.5	32.5	32.3	—
NGC 6528	33.5	32.9	32.6	32.6	33.3	33.3	32.2	32.2	33.3
NGC 6539	32.4	32.0	32.0	32.2	32.9	32.5	31.6	31.7	32.9
NGC 6569	33.6	32.5	32.7	32.9	32.8	32.9	32.2	32.5	32.8
NGC 6642	33.1	32.7	32.0	32.2	—	33.1	31.6	31.8	—
NGC 6723	33.3	31.6	32.2	32.5	32.6	32.0	31.7	32.1	32.6
NGC 6749	33.0	31.6	32.0	32.2	32.1	32.0	31.6	31.8	32.1
NGC 6809	33.1	30.6	31.3	32.1	32.0	31.0	30.9	31.7	32.0
NGC 6838	32.7	31.2	31.5	32.1	32.7	31.6	31.0	31.7	32.7
NGC 7099	33.5	32.9	32.4	32.7	—	33.3	32.0	32.3	—

(1) Calculated integrated CV X-ray luminosity within the Einstein IPC point response function. The results are scaled from 47 Tuc (columns 3 – 6) and ω Cen (columns 7 – 10). Units are $log(L_x)$, with L_x in ergs s^{-1}. An entry of "—" indicates a post-core-collapse cluster.
(2) Einstein IPC limit on point sources (Hertz & Grindlay 1983b); units are $log(L_x)$, with L_x in ergs s^{-1} over the 0.2 – 4.5 keV band.
(3) – (6) Scaling laws for CV formation: (3) equation (3.1); (4) equation (4.1); (5) by total cluster mass; (6) by cluster concentration factor (see text).

Figure Captions

Figure 1 : Stability criteria for mass transfer from a main-sequence donor star to a white dwarf of mass M_{wd}. The denominator of equation (2.2.a) is plotted vs. the mass of the donor star for three white dwarf masses and for three values of β, the parameter that specifies the fraction of the mass lost by the donor star that is accreted by the white dwarf. For positive values of the denominator, the mass transfer is stable, while for negative values it should be unstable. The specific angular momentum of the matter lost from the system has been taken to be that of the white dwarf.

Figure 2 : Evolutionary tracks for CV's with giant or subgiant companions (solid curves) and main-sequence companions (dashed curve). In all cases, the accreting white dwarf was taken to have a mass of 1.1 $M_{\odot}$, while the intial mass of the companion was 0.7 $M_{\odot}$. Angular momentum losses due to magnetic braking, the emission of gravitational radiation, and mass loss are taken into account. The filled circles indicate evolutionary times in logarithmic steps of 0.5 for times up to 10^9 years and 0.1 thereafter, starting at $10^{7.5}$ yrs. The numbers near the start and near the end of the evolutionary tracks for systems with giant companions represent the mass of the degenerate He core in units of $M_{\odot}$.

Figure 3 : Luminosity vs. orbital period at the current epoch for CVs that were formed via two-body tidal capture in 47 Tuc [panel (a)] and in ω Cen [panel (b)]. Each dot or open circle represents a binary system. In order to enhance the statistical presentation, we show approximately 100 times as many systems as are expected to be in each cluster. Systems with longer orbital periods ($\sim 5-1000$ hours) have giant or subgiant companions. Systems in the inverted "L" shaped regions have main-sequence companions and are in the post "period-gap" phase (see text). The open circles with $\sim 3 < P_{orb} < 5$ hours have main-sequence companions which have not yet entered the period gap.

Figure 4 : Calculated distribution of luminosities for binary systems containing accreting white dwarfs that were formed via two-body tidal capture in 47 Tuc.

(a) Distribution of X-ray luminosities where the conversion from accretion luminosity to X-ray (0.5 - 4 keV) luminosity is made utilizing the prescription of Patterson & Raymond (1985). The hatched curve is a smoothed version of the actual calculated luminosity distribution; this deemphasizes peaks in the distribution which result largely from the discrete values of the masses of the white dwarfs in the calculations and the use of the Patterson & Raymond prescription.

(b) Distribution of accretion luminosities ($L_{acc} = GM\dot{M}/R$)

(c) and (d) Integrated cluster luminosity from 47 Tuc as a function of source luminosity, corresponding to (a) and (b), respectively.

Figure 5 : Calculated distribution of luminosities for binary systems containing accreting white dwarfs that were formed via two-body tidal capture in ω Cen. Other descriptors are the same as in Figure 4.

Figure 6 : Calculated distribution of orbital periods for binary systems containing accreting white dwarfs that were formed via two-body tidal capture in 47 Tuc.

(a) Distribution of orbital periods for systems with *X-ray luminosities* $> 10^{29}$ ergs s^{-1} (filled circles; this essentially includes all systems) and $> 10^{31}$ ergs s^{-1} (open circles). These two curves coincide for orbital periods > 3 hours. The X-ray luminosities used to form this distribution were computed with the Patterson & Raymond (1985) prescription (see text).

(b) Same as in (a) except that the two curves are for *accretion luminosities* $> 10^{31}$ ergs s^{-1} and $> 10^{33}$ ergs s^{-1}, respectively.

Figure 7 : Calculated distribution of orbital periods for binary systems containing accreting white dwarfs that were formed via two-body tidal capture in ω Cen. Other descriptors are the same as in Figure 6.

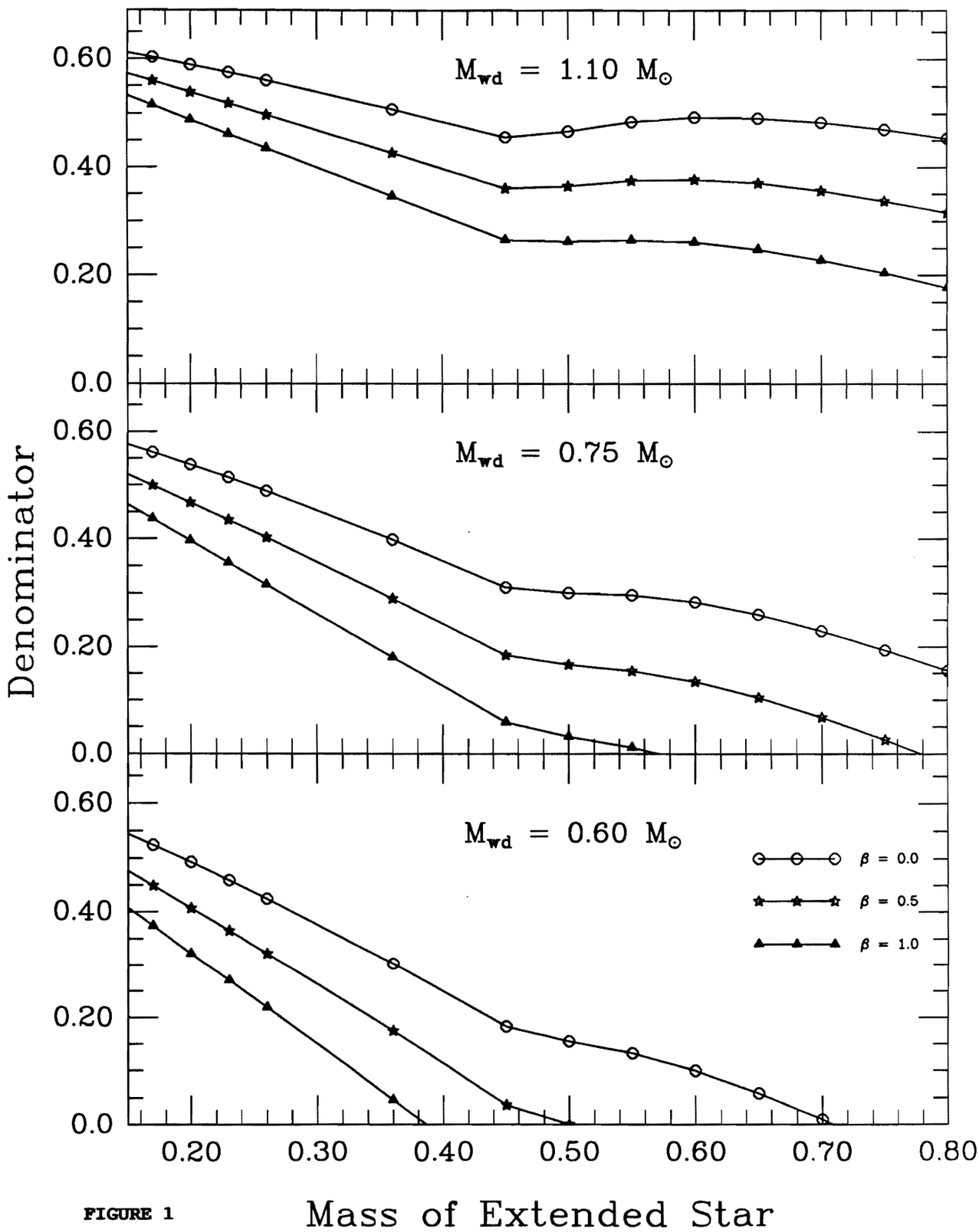
Denominator
0.60
0.40
0.20
0.0
M_{wd} = 1.10 $M_\odot$
M_{wd} = 0.75 $M_\odot$
M_{wd} = 0.60 $M_\odot$
β = 0.0
β = 0.5
β = 1.0
0.20
0.30
0.40
0.50
0.60
0.70
0.80
Mass of Extended Star

FIGURE 1

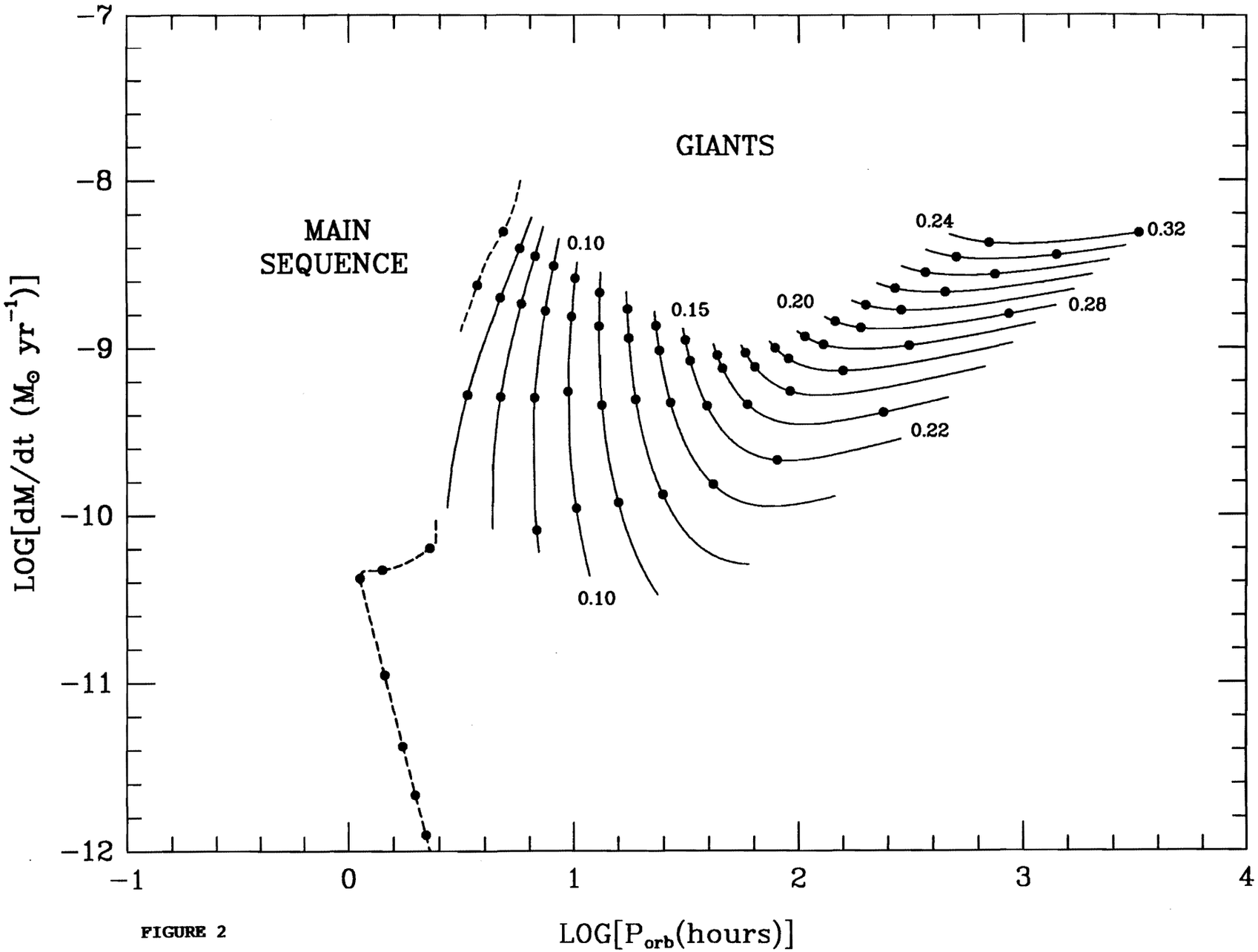
GIANTS
MAIN SEQUENCE
0.10
0.10
0.15
0.20
0.22
0.24
0.28
0.32
LOG[dM/dt (M⊙ yr⁻¹)]
LOG[P_orb(hours)]
−7
−8
−9
−10
−11
−12
−1
0
1
2
3
4

FIGURE 2

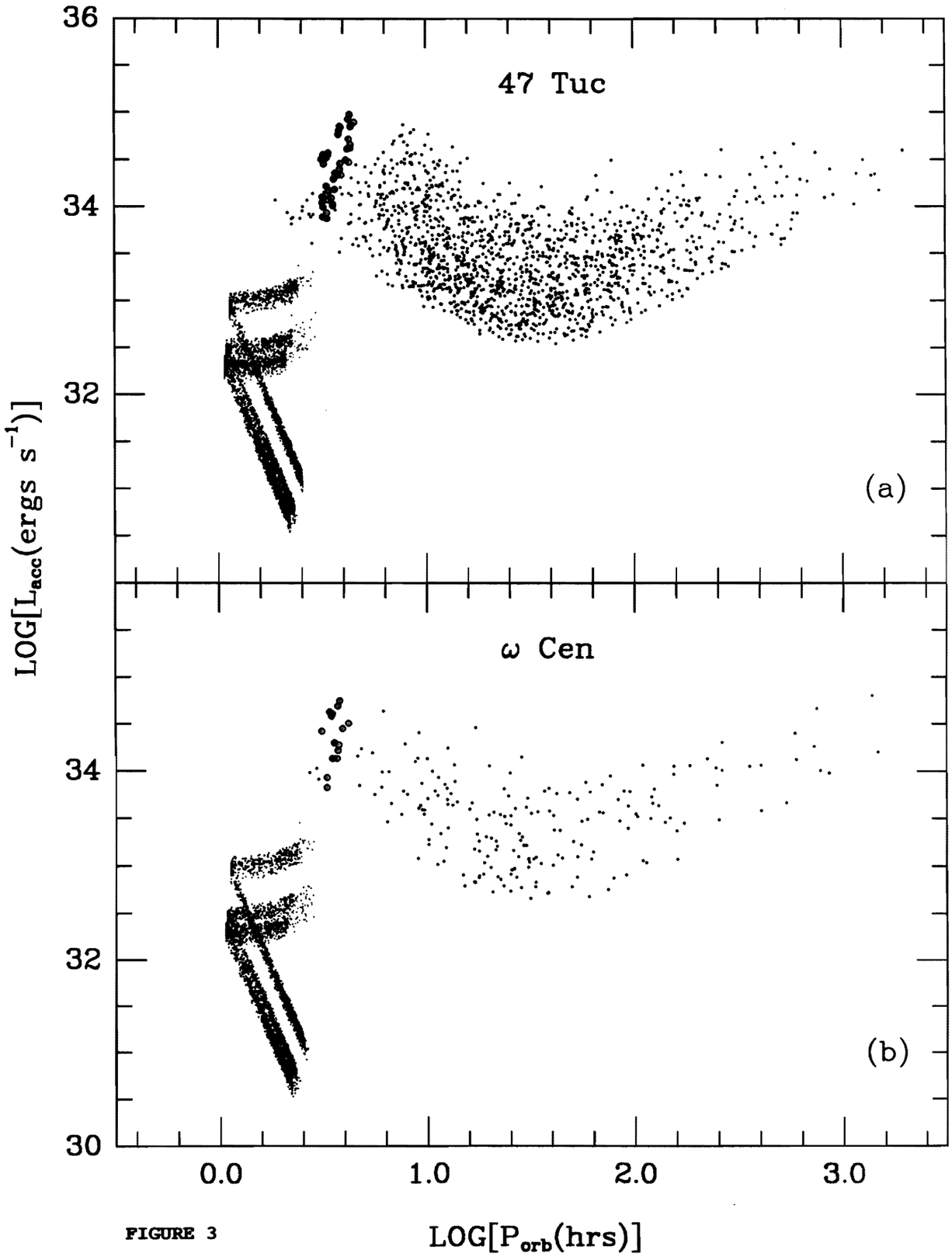
47 Tuc
(a)
ω Cen
(b)
36
34
32
34
32
30
0.0
1.0
2.0
3.0
LOG[L_acc(ergs s^-1)]
LOG[P_orb(hrs)]

FIGURE 3

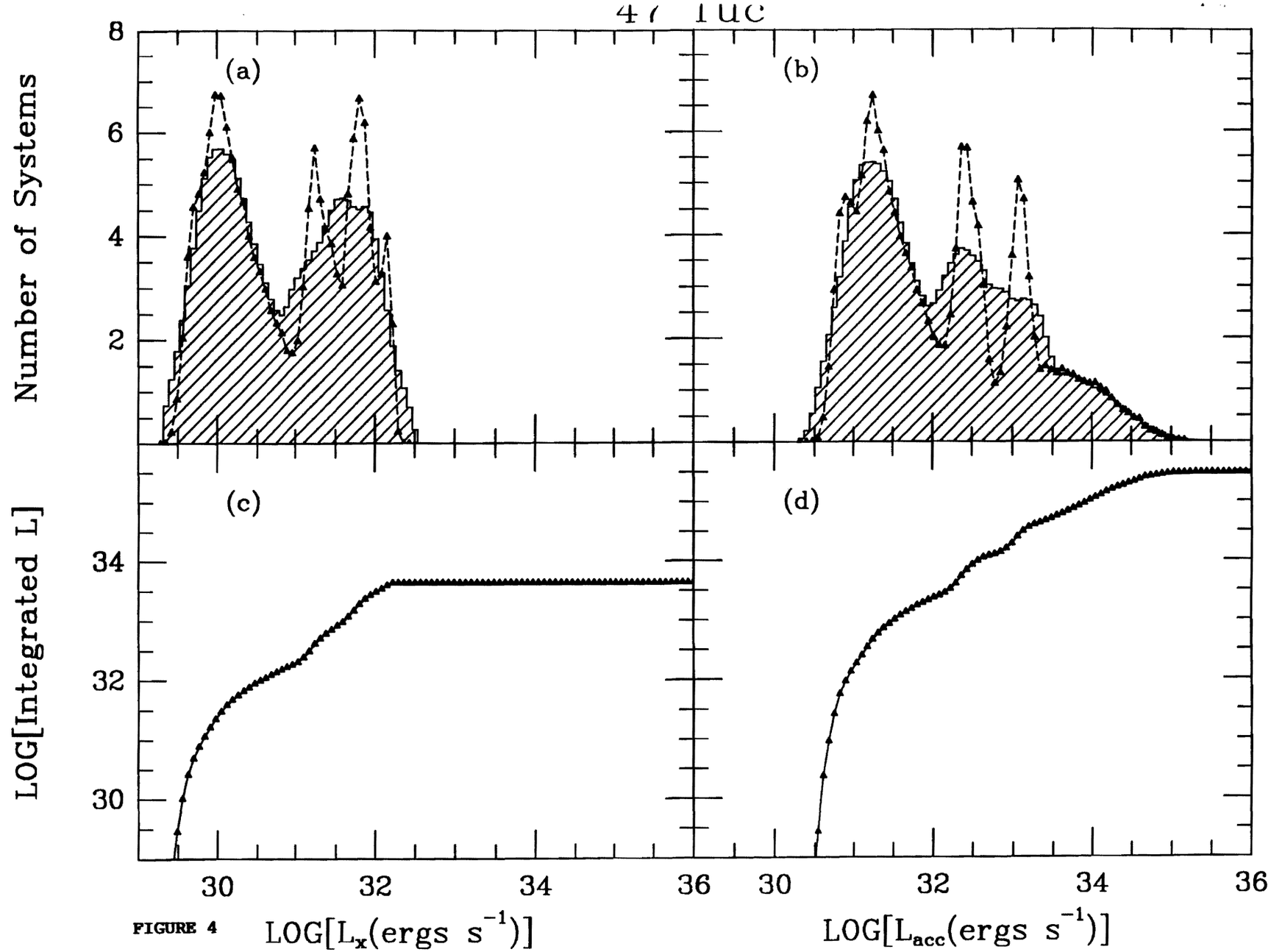
47 Tuc
(a)
(b)
(c)
(d)
Number of Systems
LOG[Integrated L]
8
6
4
2
34
32
30
30
32
34
36
LOG[L_x(ergs s^{-1})]
LOG[L_{acc}(ergs s^{-1})]

FIGURE 4

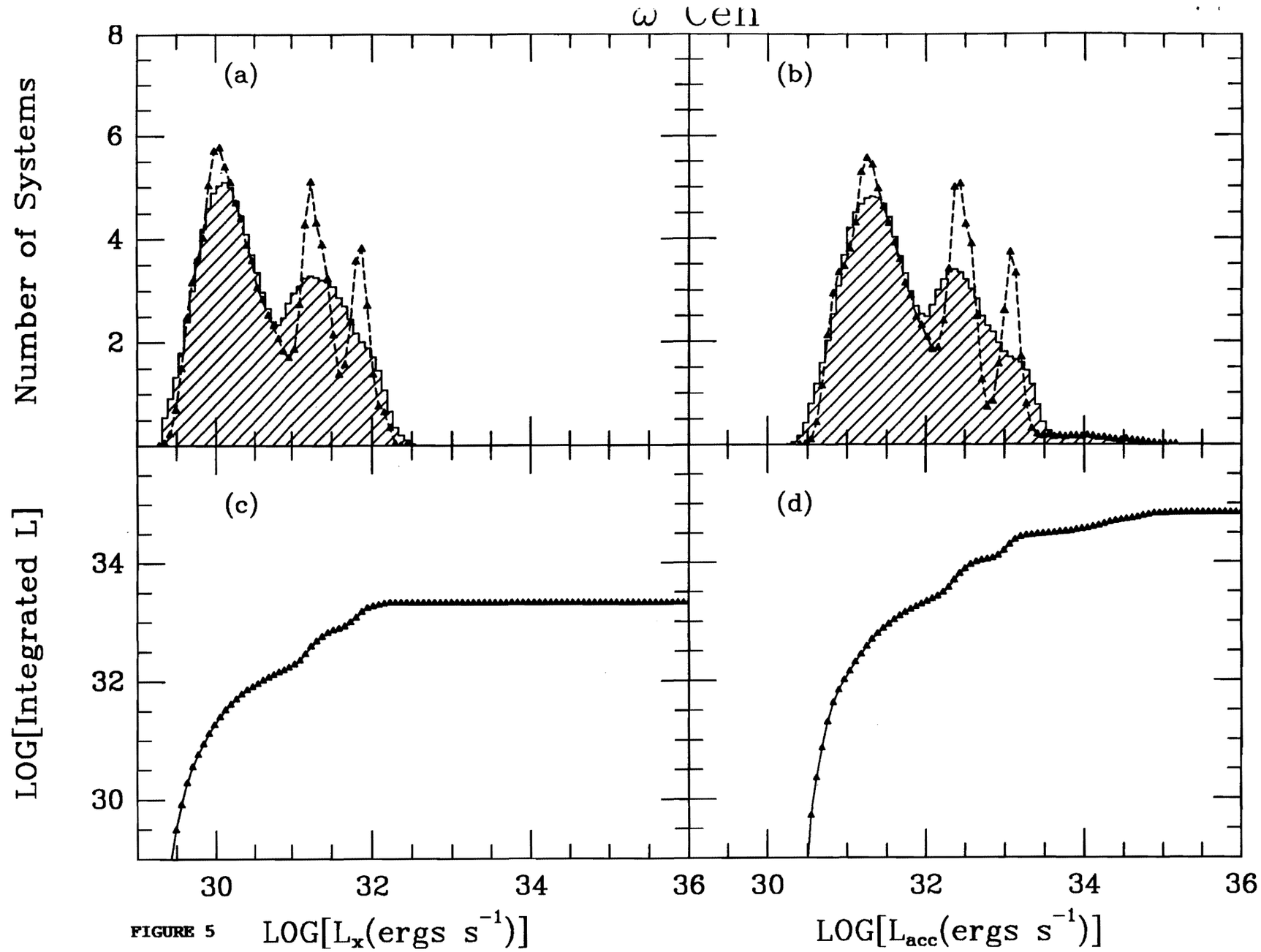
ω Cen
(a)
(b)
(c)
(d)
Number of Systems
LOG[Integrated L]
8
6
4
2
34
32
30
30
32
34
36
LOG[L_x(ergs s^-1)]
LOG[L_acc(ergs s^-1)]

FIGURE 5

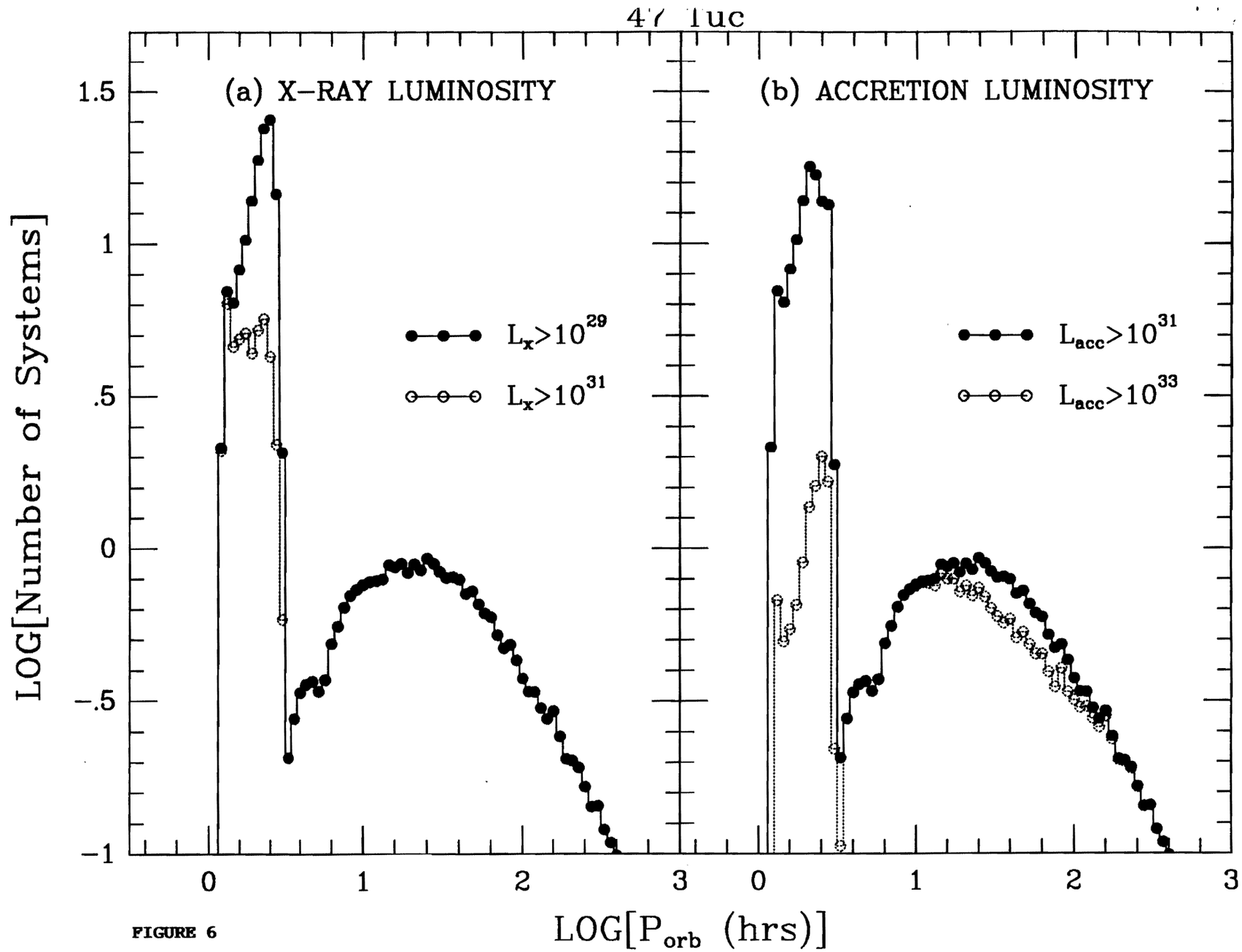
47 Tuc
(a) X-RAY LUMINOSITY
(b) ACCRETION LUMINOSITY
$L_x>10^{29}$
$L_x>10^{31}$
$L_{acc}>10^{31}$
$L_{acc}>10^{33}$
LOG[Number of Systems]
LOG[P_{orb} (hrs)]
1.5
1
.5
0
−.5
−1
0
1
2
3

FIGURE 6

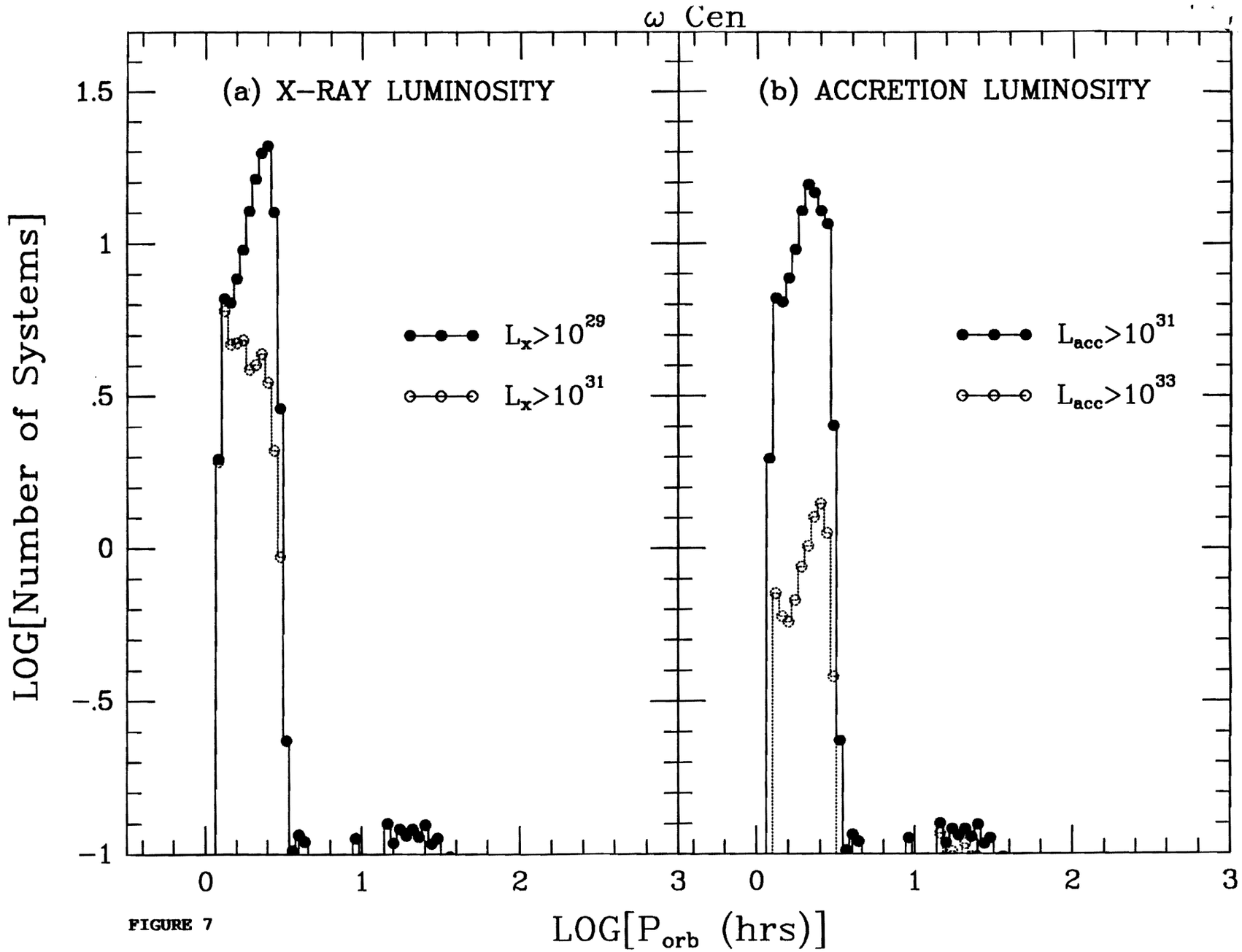
ω Cen
(a) X-RAY LUMINOSITY
(b) ACCRETION LUMINOSITY
$L_x>10^{29}$
$L_x>10^{31}$
$L_{acc}>10^{31}$
$L_{acc}>10^{33}$
LOG[Number of Systems]
LOG[P_{orb} (hrs)]
1.5
1
.5
0
−.5
−1
0
1
2
3

FIGURE 7